WAPD-TM-145

AEC RESEARCH AND
DEVELOPMENT REPORT

F0020 - AN IBM-704 THERMAL TRANSIENT ANALYSIS CODE

JANUARY 1959

Contract AT-11-1-GEN-14

BETTIS PLANT—PITTSBURGH, PA. OPERATED FOR THE
U.S. ATOMIC ENERGY COMMISSION BY BETTIS ATOMIC
POWER DIVISION, WESTINGHOUSE ELECTRIC CORPORATION

DISCLAIMER

WAPD-TM-145
UC-34: Physics and Mathematics
TID-4500 (14th Ed.)

F0020 — AN IBM-704 THERMAL TRANSIENT ANALYSIS CODE

J. B. Callaghan • J. S. Williams, Jr.

Contract AT-11-1-GEN-14

January 1959

Price $1.25
Available from the Office of Technical Services,
Department of Commerce,
Washington 25, D. C.

BETTIS PLANT • PITTSBURGH, PA.
OPERATED FOR THE U.S. ATOMIC ENERGY COMMISSION BY
BETTIS ATOMIC POWER DIVISION, WESTINGHOUSE ELECTRIC CORPORATION

LEGAL NOTICE

STANDARD EXTERNAL DISTRIBUTION

	No. of Copies
UC-80: Reactors—General, TID-4500, 14th Edition	594

SPECIAL EXTERNAL DISTRIBUTION

Manager, Pittsburgh Naval Reactors Operations Office, AEC	3
Pittsburgh Naval Reactors Operations Office W. Katsur	5
Aerojet-General Corporation K. Sato	1
Argonne National Laboratory D. A. Flanders, P. Lottes	3
Babcock and Wilcox Company H. F. Dobel, J. Mumm	2
Battelle Memorial Institute J. W. Chastain	1
Brookhaven National Laboratory J. Chernick, M. Rose	2
California Institute of Technology R. Sabersky	1
Columbia University A. J. Bendler	1
Combustion Engineering, Inc. L. E. Anderson, S. Visner	3
David Taylor Model Basin H. Polachek	2
General Electric Atomic Power Equipment Department E. Polomik	1
Hanford Atomic Products Operation J. M. Batch	1
Knolls Atomic Power Laboratory R. Ehrlich, G. Halsey, R. J. Hoe	12
Los Alamos Scientific Laboratory B. Carlson	2
Massachusetts Institute of Technology P. Griffith	1
Mine Safety Appliance Research Corporation E. C. King, J. McDonough, W. Milich	3
New York University R. Richtmyer	2
Oak Ridge National Laboratory A. Householder	2
Purdue University R. J. Grosch	1
Ramo-Woolridge Corporation N. Zuber	1
Rocketdyne Propulsion Field Laboratory R. Mascolo	1
Stanford University W. M. Kays, G. Leppert	1
University of California V. E. Schrock	1
University of California at Los Angeles Y. Chang, K. Forster, M. Tribus	3
University of California Radiation Laboratory, Livermore S. Fernbach	2
University of Illinois J. W. Westwater	1
University of Michigan J. A. Clark	1
University of Minnesota N. R. Amundson	1
University of Pittsburgh G. Sonnemann	1
Westinghouse Atomic Power Department A. Thorpe	1
Westinghouse Research Laboratories R. D. Cess, E. Somers, S. Way	3
TOTAL	660

THIS PAGE

WAS INTENTIONALLY

LEFT BLANK

CONTENTS

An IBM-704 thermal transient analysis code, designated F0020, has been developed to reduce transient test data for a single, vertical, rectangular coolant channel. Modes of heat transfer to water at 2000 psia covered by this code include: (1) forced convection (turbulent flow), (2) nucleate boiling, (3) departure from nucleate boiling, (4) partial film boiling, and (5) film boiling. The code will accommodate a plate mesh, and associated heat generation weighting factors, of a maximum of 50 axial and 10 radial nodes.

F0020—AN IBM-704 THERMAL TRANSIENT ANALYSIS CODE

J. B. Callaghan and J. S. Williams, Jr.

SUMMARY

An IBM-704 digital computer code has been developed to reduce thermal transient test data. The code is available for use under the Bettis Fortran code number F0020.

The code numerically solves the partial differential plate equation

$$\rho_m C_{pm} \frac{\partial T_m}{\partial \tau} = K_m \frac{\partial^2 T_m}{\partial X^2} + q'''$$

and the fluid equations

$$W \frac{\partial h}{\partial z} = 2\delta\phi - \rho A_F \frac{\partial h}{\partial \tau} ,$$

$$\frac{\partial W}{\partial z} = - A_F \frac{\partial \rho}{\partial \tau} ,$$

and

$$- \frac{\partial P}{\partial z} = \frac{1}{144g} \left[\frac{\partial}{\partial z} \left(\frac{G^2}{\rho} \right) + \frac{\partial G}{\partial \tau} + g\rho + \frac{fG^2}{2D_H\rho} \right]$$

for a single, vertical, rectangular coolant channel model.

F0020 can include the following modes of heat transfer for a typical analysis:

1) Forced convection (turbulent flow)
2) Nucleate boiling
3) Departure from nucleate boiling
4) Partial film boiling
5) Film boiling

The boundary conditions for surface heat transfer were derived from empirical steady state correlations for water at 2000 psia pressure.

The input forcing functions are:

1) $W_{il} = \frac{W_{ol}}{1 + b\tau'}$ (instantaneous inlet flow),

2) $h_{il} = h_{ol} + c\tau'$ (instantaneous inlet enthalpy),

and

3) $\bar{I}_i = \bar{I}_o + d\tau' + e(\tau')^2$ (instantaneous average current).

For reactor application, the heat generation can be expressed in terms of $\bar{I}_i$.

The output includes plate temperatures at selected axial and radial nodes and water conditions at selected axial nodes. The over-all pressure drop is also an output. F0020 will accommodate a plate mesh, and associated heat generation weighting factors, of a maximum of 50 axial and 10 radial nodes.

The code has shown satisfactory solution stability for typical reactor loss-of-coolant-flow accident test cases. Other types of reactor accidents have not been simulated with F0020.

INTRODUCTION

As early as 1956, the status of pressurized water reactor design indicated the need for experimental information on transient tests to evaluate any difference between steady state and transient departure from nucleate boiling (hereinafter referred to as DNB) and pressure drop. For some reactors, the limiting thermal design condition may occur during a transient such as a loss-of-coolant flow accident. Aside from the considerable effort required to develop a test apparatus capable of measuring transient conditions, a parallel effort was necessary to establish a suitable method of analyzing the forthcoming data.

The transient analysis of the thermal and hydraulic interaction between a solid heat source and a fluid heat sink is difficult because the interface boundary conditions are a function of the solid surface temperature and/or the local fluid enthalpy. For pressurized water reactor application, the problem is further complicated if the analysis must include a change of phase of the coolant. To date, no sufficiently general, closed-form solution has been found for the equations governing such a system. However, the advent of modern high speed computing equipment has made practical the solution of problems of this type by numerical approximation methods.

It was decided that the analysis of the test data would attempt to describe the system with imposed forcing functions (to be determined from the testing) of inlet flow, inlet enthalpy, and average test section heat generation as a function of time. The calculated element and fluid responses would then be compared with corresponding measured quantities obtained from the tests. Existing analytical methods, such as dynamic analog simulation (Ref 1) and digital codes (Ref 2), could not be utilized for this analysis. F0020, as described in the following sections, was formulated to solve this problem.

PROBLEM MODEL

F0020 uses the equations and boundary conditions given in this section as the problem model. Obvious limitations are presented as a conclusion to the section.

Differential Equations

The governing equations for the physical model of a single, vertical, rectangular coolant channel (Fig. 1) have been derived and are set forth below:

Plate Heat Audit

$$\rho_m C_{pm} \frac{\partial T_m}{\partial \tau} = K_m \frac{\partial^2 T_m}{\partial x^2} + q'''(x,\tau) \tag{1}$$

Fluid Enthalpy

$$W \frac{\partial h}{\partial z} = 2\delta\phi - \rho A_F \frac{\partial h}{\partial \tau} \tag{2}$$

Fluid Continuity

$$\frac{\partial W}{\partial z} = - A_F \frac{\partial \rho}{\partial \tau} \tag{3}$$

Fluid Pressure Drop

$$- \frac{\partial P}{\partial z} = \frac{1}{144g} \left[\frac{\partial}{\partial z} \left(\frac{G^2}{\rho} \right) + \frac{\partial G}{\partial \tau} + g\rho + \frac{f G^2}{2 D_H \rho} \right] \tag{4}$$

The treatment of W, ρ, and h in Eqs (2), (3), and (4) assumes a single spatial dimensional (z) variation. This assumption is necessary because of the lack of a good multi-spatial-dimension model. Further, the transient test apparatus was designed to measure only coolant and wall temperatures in the axial direction. Equation (2) results from the additional assumption that $\partial P/\partial \tau$ is negligible. This assumption simplifies the calculation procedure by uncoupling the thermodynamic and dynamic equations.

Equation (1) is the standard one-dimensional Fourier conduction equation for constant ρ_m, C_{pm}, and K_m. This equation is used in F0020 to compute the plate temperature profile in the plate thickness direction (x direction of Fig. 1) at discrete axial (z) locations. Preliminary studies of the solution of the more rigorous plate equation

$$\rho_m(T_m)\, C_{pm}(T_m) \frac{\partial T_m}{\partial \tau} = \frac{\partial}{\partial x} K(T_m) \frac{\partial T_m}{\partial x} + q'''(x,\tau) \tag{5}$$

indicated that the small error involved in using Eq (1) at any fixed axial location did not warrant the increased code complexity necessary to use Eq (5).

Finite Difference Representation

The original reduction of the differential equations to finite difference form suitable for digital solution was performed by Dr. N. R. Amundson of the University of Minnesota. With minor modification, the F0020 fluid equations are as originally reduced. The plate equations have undergone considerable evolution to insure solution stability for all conditions of heat transfer considered by the code. The F0020 representation of Eqs (1)-(4) is given below. (The derivation of these equations is given in Appendix II.)

Plate Conduction Equations

The plate conduction equations involve three variables: a time instant, i; an axial location, j; and a radial node, k. The physical model is shown in Fig. 2. The equations are as follows. [The m (metal) subscript has been dropped for simplicity.]

1) For internal (K^{th}) node ($2 \leq K \leq x - 1$)

$$T_{ijk} = \frac{1}{3} \left[T_{i-1,j,k-1} + T_{i-1,jk} + T_{i-1,j,k+1} \right] + \frac{q'''_{ijk}\, \Delta\tau}{\rho C_p} \tag{6}$$

2) For last (X^{th}) node ($3 \leq x \leq 10$)

$$T_{ijx} = \frac{1}{3} \left[T_{i-1,j,x-1} + 2\, T_{i-1,jx} \right] + \frac{q'''_{ijx}\, \Delta\tau}{\rho C_p} \tag{7}$$

3) For thermocouple (TC) node

$$T_{ijTC} = \frac{1}{3}\left[T_{i-1,j,x-1} - T_{i-1,jx} + 3\,T_{i-1,jTC}\right] + \frac{q'''_{ijx}\,\Delta\tau}{\rho C_p} \tag{8}$$

4) For first (1^{st}) node

a) Forced convection and nucleate boiling:

$$T_{ij1} = \frac{1}{3}\left[T_{i-1,j2} + 2\,T_{i-1,js}\right] + \frac{q'''_{ij1}\,\Delta\tau}{\rho C_p} \tag{9}$$

b) DNB, partial film boiling, and film boiling:

$$T_{ij1} = X\,\overline{T}_{ij} - T_{ij2} - T_{ij3} \cdots T_{ijx} \tag{10}$$

5) For surface, s, node

a) Forced convection:

$$T_{ijs} = \left[1 - \frac{H_{ij}\Delta\tau}{\rho C_p \Delta x}\right] T_{i-1,js} + \frac{1}{3}\left[T_{i-1,j2} - T_{i-1,j1}\right] + \left[\frac{H_{ij}\Delta\tau}{\rho C_p \Delta x}\right] T_{wij} + \frac{q'''_{ij1}\,\Delta\tau}{\rho C_p} \tag{11}$$

b) Local boiling:

$$T_{ijs} \equiv T_{scrit} \tag{12}$$

c) DNB, partial film boiling, and film boiling:

$$T_{ijs} = T_{i-1,js} + T_{ij1} - T_{i-1,j1} \tag{13}$$

6) Average plate temperature

a) Forced convection and nucleate boiling:

$$\overline{T}_{ij} = \frac{1}{x}\left[T_{ij1} + T_{ij2} \cdots\cdots T_{ijx}\right] \tag{14}$$

b) DNB, partial film boiling, and film boiling:

$$\overline{T}_{ij} = \left[\sum_{k=1}^{x} (q'''_{ijk}\Delta x) - \phi_{ij}\right] \frac{\Delta\tau}{\rho C_p Y} - \overline{T}_{i-1,j} \tag{15}$$

7) Fourier modulus in node equations

$$\frac{(\Delta x)^2}{\alpha \Delta\tau} \equiv 3 \tag{16}$$

Fluid Equations

The following fluid equations include the time variable, i, and the axial location, j, ($2 < j < 50$). The physical model is shown in Fig. 3.

1) Enthalpy

$$h_{ij} = \left[\frac{W_{ij}}{\Delta z} + \frac{A_F \rho_{i-1,j}}{\Delta\tau}\right]^{-1} \left[\frac{W_{ij}}{\Delta z} h_{ij-1} + \frac{A_F \rho_{i-1,j}}{\Delta\tau} h_{i-1,j} + a\delta(\phi_{i-1,j} + \phi_{i-1,j-1})\right] \tag{17}$$

The term "a" in Eq (17) is a fluid heat pickup correction term to allow various flow-flux models to be used. The following model will be used for Bettis test data reduction. Figure 4a shows a Bettis test specimen cross-section. Approximately 95% of the total heat generation occurs in the region δY. It is assumed that the one-dimensional equations (1)-(4) are valid in this region. Figure 4b shows the code representation of the test specimen. Because the outside periphery of the

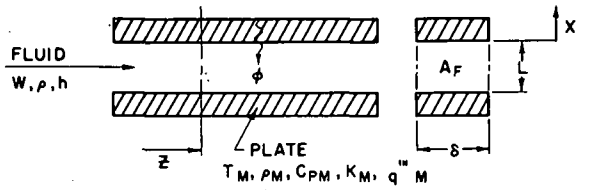

Fig. 1 Model for Derivation of Differential Equations

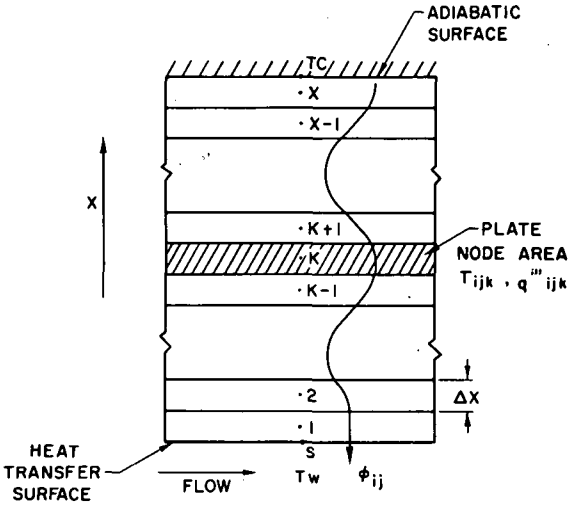

Fig. 2 (Right) One-Dimensional Plate Representation at Axial Node j and Time i

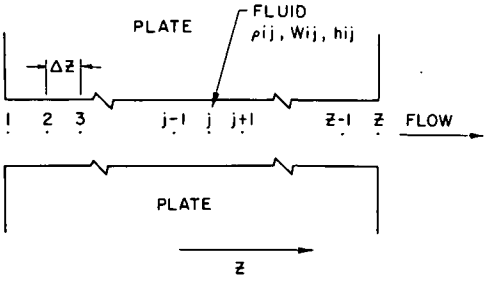

Fig 3 One-Dimensional Fluid Representation at Time i

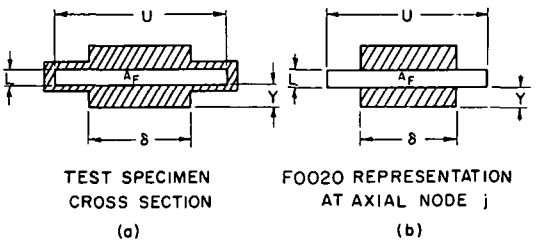

Fig. 4 Test Model and F0020 Representation

specimen is insulated, 100% of the heat generated is assumed to enter the water. For the complete fluid mixing model, which is consistent with Bettis steady-state DNB data reduction, the flow area, A_F, equals UL, and the flux area equals δL. The transient flux and coolant heat pickup are approximated by:

a) reducing the over-all measured generation to 95% as input in Eq (23);

b) accounting for the end channel heat pickup by making "a" in Eq (17) equal to 1/0.95.

Physically, this is equivalent to the assumption that the ratio of end channel flux to generating width channel flux is the same in the transient as in the steady state.

The no-fluid mixing model, such as might be used for reactor design purposes, would use a = 1.00 and $A_F = \delta L$ with the corresponding generation that occurs in plate width δ.

2) Continuity

$$W_{ij} = W_{ij-1} - \frac{A_F \Delta z}{\Delta \tau} [\rho_{ij-1} - \rho_{i-1,j-1}] \tag{18}$$

3) Pressure drop (positive ΔP denotes a decrease in pressure from inlet to point j)

a) Frictional pressure drop:

$$\Delta P_{f_{ij}} = \frac{1}{288\, D_H g A_F^2} \sum_{\eta=2}^{j} \frac{\Delta z}{2} \left(\frac{f_{i\eta} W_{i\eta}^2}{\rho_{i\eta}} + \frac{f_{i\eta-1} W_{i\eta-1}^2}{\rho_{i\eta-1}} \right) \tag{19}$$

b) Time acceleration pressure drop:

$$\Delta P_{T_{ij}} = \frac{1}{144\, A_F g \Delta\tau} \sum_{\eta=2}^{j} \frac{\Delta z}{2} \left[W_{i\eta} - W_{i-1,\eta} + W_{i\eta-1} - W_{i-1,\eta-1} \right] \tag{20}$$

c) Spatial acceleration pressure drop:

$$\Delta P_{A_{ij}} = \frac{1}{144\, g A_F^2} \sum_{\eta=2}^{j} \left[\frac{W_{i\eta}^2}{\rho_{i\eta}} - \frac{W_{i\eta-1}^2}{\rho_{i\eta-1}} \right] \tag{21}$$

d) Elevation pressure drop:

$$\Delta P_{E_{ij}} = \frac{1}{144} \sum_{\eta=2}^{j} \frac{\Delta z}{2} \left(\rho_{i\eta} + \rho_{i\eta-1} \right) \tag{22}$$

e) Total pressure drop:

$$\Delta P_{Total_{ij}} = \Delta P_{f_{ij}} + \Delta P_{T_{ij}} + \Delta P_{A_{ij}} + \Delta P_{E_{ij}} \tag{23}$$

Input Forcing Functions

The code requires the following input forcing functions:

1) Instantaneous inlet flow:

$$W_{i1} = \frac{W_{o1}}{1 + b\tau'} \tag{24}$$

2) Instantaneous inlet enthalpy:

$$h_{i1} = h_{o1} + c\tau' \tag{25}$$

3) Instantaneous average current:

$$\bar{I}_i = \bar{I}_o + d\tau' + e(\tau')^2 \tag{26}$$

The average current is related to the average heat generation rate by the equation

$$\bar{q}_i''' = \frac{M \rho_E}{4\, A_P^2} \left[\frac{\bar{I}_i}{N_F} \right]^2 \tag{27}$$

The individual node generation rate is expressed as

$$\bar{q}_{ijk}''' = \bar{q}_i''' F_j F_k \ . \tag{28}$$

The representation assumes a spatially separable generation profile independent of time. The F_k term allows nongenerating and generating radial region (such as fuel and clad in reactors) calculation, and the F_j term accommodates a nonuniform axial generation profile.

The constants b, c, d, and e of Eqs (24)-(26) are experimentally determined for each test.

Boundary Conditions and Assumptions

The following boundary conditions and assumptions are imposed on the code solution.

1) General: The solution will proceed from a known steady state condition existing immediately prior to the start of the transient.

2) Plate:

   a) The plate quantities ρ_m, C_{pm}, K_m, and ρ_E are represented at all nodes by the same values; i.e., they are not expressed as a function of temperature.

b) The plate heat flow in the axial direction is negligible.

c) The surface represented by the TC node in Fig. 2 is adiabatic.

d) The instantaneous generation rate is known for all times at each node.

3) Fluid

a) The fluid within the flow area, A_F, at any axial location is represented by a single condition; no radial variation of properties exist.

b) The channel fluid inlet flow and enthalpy are known for all times.

c) The coolant is water at a system pressure of 2000 psia. (With minor modification, the pressure dependent code constants can be changed.)

d) The system base pressure variation with time, $\partial P/\partial \tau$, is negligible.

4) Plate-fluid interface heat flux: The heat flux at the plate-fluid interface will be as shown in Fig. 5. This figure identifies five regions of heat transfer, as follows:

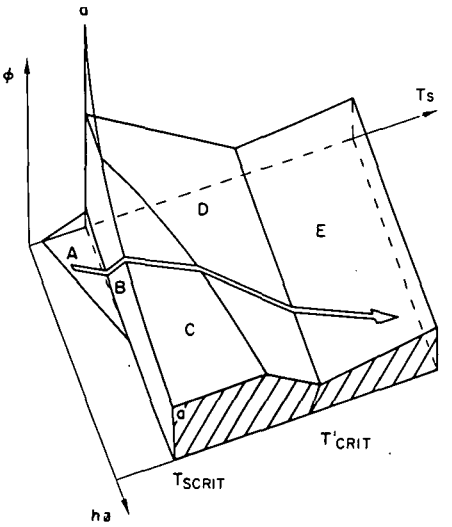

⇨ WALL TEMPERATURE PROGRESSION FOR A LOSS OF PUMPING POWER ACCIDENT

A - FORCED CONVECTION
B - NUCLEATE BOILING
C - DEPARTURE FROM NUCLEATE BOILING
D - PARTIAL FILM BOILING
E - FILM BOILING

Fig. 5 Heat Transfer Boundary Condition Representation for F0020

a) Forced convection (Region A, Fig. 5): This heat transfer mechanism occurs when $T_{ijs} < T_{scrit}$. At 2000 psia, T_{scrit} has a weak flux dependency which is neglected in F0020. The approximate value of T_{scrit} is determined from the Jens and Lottes (Ref 4) correlation

$$T_{scrit} = T_{sat} + \frac{60(\phi)^{1/4}}{e_o(P/900)} \tag{29}$$

for the anticipated average flux existing for the particular problem. For this region,

$$\phi_{ij} = H_{ij}(T_{ijs} - T_{ijw}) \ , \tag{30}$$

where H_{ij} is derived from the Dittus-Boelter (Ref 5) relationship

$$N_{Nu} = 0.023\, N_{Re}^{0.8}\, N_{Pr}^{0.4} \tag{31}$$

where all fluid properties are based on bulk temperature. This is expressed as follows:

$$H_{ij} = F_{ij}\left[\frac{G_{ij}}{10^6}\right]^{0.8}\left[D_H\right]^{-0.2} \tag{32}$$

$$*F_{ij} = 466.48010 + 3.1162878\, h_{ij} - 0.0023830320\, (h_{ij})^2 \text{ (for } h_{ij} \leq 600) \tag{33}$$

$$F_{ij} = 584.0 + 1.49\, h_{ij} \text{ (for } h_{ij} > 600) \tag{34}$$

b) Nucleate boiling (Region B, Fig. 5): Nucleate boiling begins when $T_{ijs} = T_{scrit}$ as approximated by Eq (29) and the flux is less than the DNB flux. For this heat transfer region,

---

* The constants for the empirical data curve fits were obtained from digital computer correlation routines. The basic information used in these routines was not known to 8 decimal places. However, because F0020 has an 8 place numerical format, the curve fits were not rounded off.

$$\phi_{ij} = \sum_{k=1}^{x} (q'''_{ijk} \Delta X) - \frac{\rho C_p Y}{\Delta \tau} [T_{ij} - T_{i-1,j}] \quad , \tag{35}$$

which is a rearrangement of Eq (15).

c) DNB and partial film boiling (Regions C and D, Fig. 5): These modes of heat transfer exist when $T_{scrit} < T_{ijs} < T'_{crit}$. The temperature at which pure film boiling begins, T'_{crit}, is an input parameter. Referring to Fig. 5, the burnout region C is generated by cutting the region D plane at the flux equal to the burnout correlation (a-a in Fig. 5). This correlation is the upper flux limit of the nucleate boiling region B.

The flux for region C (DNB) is determined from Bettis correlations (Ref 6). The code representation is

$$\frac{\phi_{ij}}{10^6} = 0.5 \left[\frac{h_{ij}}{1000} \right]^{-2.5} \left[e_o^{(-0.0024\, z_j/D_H)} \right] \text{(for } G_{ij} \leq 1.6 \times 10^6) \tag{36}$$

and

$$\frac{\phi_{ij}}{10^6} = 0.37 \left[\frac{h_{ij}}{1000} \right]^{-2.5} \left[e_o^{(-0.0024\, z_j/D_H)} \right] \left[1 + \frac{G_{ij}}{10^7} \right]^2 \text{(for } G_{ij} > 1.6 \times 10^6) \quad . \tag{37}$$

Thus, in region C, the flux level, ϕ, is not a function of T_s.

The flux for region D (partial film boiling) is determined from Mine Safety Appliance Research data (Ref 7). The data were limited in range in the h_z dimension (enthalpy) of Fig. 5. Therefore, the functional form suggested by these data was utilized, but the constants are retained as input information. The flux for region D is

$$\phi_{ij} = A - B[T_{i-1js}] \quad . \tag{38}$$

When $T_{scrit} < T_{ij} < T'_{crit}$, the ϕ_{ji} is found by computing ϕ_{ij} from either Eq (36) or (37) and from Eq (38) and taking the lower of the two values.

As shown in Fig. 5, the transition from nucleate boiling (region B) to partial film boiling (region D) is discontinuous in flux level with this model. This results from the model statement that the DNB line, a-a, represents this transition, while the flux at wall temperatures greater than T_{scrit} is the minimum value of the correlations for regions C and D. The location of this discontinuity cannot be defined for all cases because of the effect of the various parameters on the DNB flux. However, preliminary runs have indicated that temperature excursions during the Bettis out-of-pile transient tests pass through the B-C-D region without any flux discontinuity. Figure 5 indicates a typical wall temperature excursion through the B-C-D region.

d) Pure film boiling (region E, Fig. 5): Pure film boiling occurs when $T_{ijs} \geq T'_{crit}$. It is probable that T'_{crit} is higher than the wall temperatures currently anticipated in pressurized water reactor application. However, region E is included for completeness. This region, like regions C and D, is not well defined. The functional form, suggested from quenching tests (Ref 8) at atmospheric pressure, is

$$\phi_{ij} = C + D[T_{i-1js}] \quad , \tag{39}$$

where C and D are input information.

One further degree of freedom is provided in the representation of the heat flux boundary condition. The constants defining line a-a and region C of Fig. 5 are fixed in the code.

However, it is possible to establish indirectly new constants for Eqs (36) and (37) by the DNB time input value. The code compares the actual surface flux with the DNB flux given by Eqs (36) and (37) (line a-a of Fig. 5). It also compares the input DNB time value with the elapsed transient time. If DNB, as established by Eqs (36) and (37), has not been reached at a transient time equal to this input DNB time, the constants of these equations will be computed to adjust line a-a and region C so that DNB occurs at this input DNB time at the channel outlet node, z. If DNB has occurred at the end channel when the elapsed time equals the input DNB time, no adjustment will be made to the equations. This feature allows use of an additional piece of test information—the time to DNB, as indicated by thermocouple traces. However, its practical use may be limited to uniform axial generation cases.

5) Frictional pressure drop: The friction factor variation is included in Eq (19) by use of the f_{ij}/ρ_{ij}. With minor modification, the following F0020 representation is the same as that in Ref 9:

a) Bulk boiling ($h_{ij} > h_{sat}$):

$$f_{ij}/\rho_{ij} = f_{iso_{sat}} \Phi^2_{Lo}/\rho_{sat} \quad , \tag{40}$$

where

$$f_{iso_{sat}} = 0.2108160\ N_{Re_{sat}}^{-0.2137270} \quad (\text{for } N_{Re_{sat}} < 10^5) \quad , \tag{41}$$

$$f_{iso_{sat}} = 0.1143700\ N_{Re_{sat}}^{-0.1606080} \quad (\text{for } N_{Re_{sat}} \geq 10^5) \quad , \tag{42}$$

$$N_{Re_{sat}} = G_{ij}\ D_H/\mu_{sat} \quad , \tag{43}$$

$$\Phi^2_{Lo} = \chi_1 X_{ij} + \chi_2 \quad ,$$

$$X_{ij} = \frac{h_{ij} - 671.7}{463.4} \quad , \tag{45}$$

$$\chi_1 = a_1 + a_2 \left[G_{ij}/10^6 \right]^{-1} + a_3 \left[G_{ij}/10^6 \right]^{-2} \quad , \tag{46}$$

$$\chi_2 = a_4 + a_5 \left[G_{ij}/10^6 \right]^{-1} \quad . \tag{47}$$

The a_1 through a_5 in Eqs (46) and (47) are functions of X_{ij} and are presented in the curve fit section.

b) No bulk boiling ($h_{ij} \leq h_{sat}$):

$$f_{ij}/\rho_{ij} = f_{iso_{ij}}\ (f/f_{iso})_{ij}/\rho_{ij} \quad , \tag{48}$$

where

$$f_{iso_{ij}} = 0.2108160\ N_{Re}^{-0.2137270} \quad (\text{for } N_{Re} < 10^5) \quad , \tag{49}$$

$$f_{iso_{ij}} = 0.1143700\ N_{Re}^{-0.1606080} \quad (\text{for } N_{Re} \geq 10^5) \quad , \tag{50}$$

and

$$N_{Re} = G_{ij}\ D_H/\mu_{ij} \quad . \tag{51}$$

(1) For $\Delta T_f < \Delta T_{J\&L}$ (no nucleate boiling):

(where

$$\Delta T_{J\&L} \equiv T_{scrit} - T_{ijw} \tag{52}$$

and

$$\Delta T_f \equiv 0.766\ \phi_{ij}/H_{ij}) \tag{53}$$

$$(f/f_{iso})_{ij} = 1 - 0.0025\ \Delta T_f \tag{54}$$

$$(f/f_{iso})_{ij} = 0.85\ . \tag{55}$$

For no nucleate boiling, $(f/f_{iso})_{ij}$ is the maximum value as calculated from Eqs (54) or (55).

(2) For $\Delta T_f > \Delta T_{J\&L}$ (nucleate boiling):

$$(f/f_{iso})_{ij} = (1 - 0.0025\ \Delta T_{J\&L}\left[1 + 0.76\left(\frac{G_{ij}}{10^6}\right)^{-2/3}\left(1 - \frac{\Delta T_{J\&L}}{\Delta T_f}\right)\right] \tag{56}$$

$$(f/f_{iso})_{ij} = 0.85\left[1 + 0.76\left(\frac{G_{ij}}{10^6}\right)^{-2/3}\left(1 - \frac{\Delta T_{J\&L}}{\Delta T_f}\right)\right] \tag{57}$$

For nucleate boiling, $(f/f_{iso})_{ij}$ is the maximum value as calculated from Eqs (56) or (57).

Curve Fits

The following property representations for water at 2000 psia are used in F0020 (Refs 10-12).

1) Temperature

$$T_{ijw} = -60.977250 + 1.4437033\ h_{ij} - 0.00059984467\ (h_{ij})^2 \text{ (for } h_{ij} < h_{sat}) \tag{58}$$

$$T_{ijw} \equiv T_{sat} \text{ (for } h_{ij} \geq h_{sat}) \tag{59}$$

$$T_{sat} = 635.78 \tag{60}$$

$$h_{sat} = 671.7 \tag{61}$$

2) Density

$$\rho_{ij} = 59.804439 + 0.005334730\ h_{ij} - 0.000053630137\ (h_{ij})^2 \text{ (for } h_{ij} < h_{sat}) \tag{62}$$

$$\rho_{ij} = (0.000349806\ h_{ij} - 0.0209265)^{-1} \text{ (for } h_{ij} \geq h_{sat}) \tag{63}$$

3) Viscosity

$$\mu_{ij} = 1.6015870 - 0.0062619952\ h_{ij} + 0.0000077597482\ (h_{ij})^2 \text{ (for } h_{ij} < 370) \tag{64}$$

$$\mu_{ij} = 0.7537780 - 0.0014881633\ h_{ij} + 0.00000098193168\ (h_{ij})^2 \text{ (for } h_{ij} \geq 370) \tag{65}$$

$$\mu_{sat} = 0.192 \tag{66}$$

4) The values for the constants of the Φ_{Lo}^2 term in the quality frictional pressure drop are as follows:

	$X_{ij} \leq 0.06$	$0.06 < X \leq 0.20$	$X > 0.20$
a_1	1.9034337	0.0688607	-0.0457867
a_2	8.5584910	6.1889560	3.0925460
a_3	2.7912118	3.0285472	3.9200889
a_4	1.0000000	1.0960000	1.2320000
a_5	0.0000000	0.1429000	0.4206000

SOLUTION SEQUENCE

Two solution sequences are of general interest. These are the over-all fluid-plate solution sequence and the sequence of calculation of plate surface heat flux. The code procedure covering these items is as follows.

Over-All Fluid-Plate Solution Sequence

The practical difficulty of deriving the fluid equations (17)-(23), is connected with the establishment of a working extrapolation procedure, which is shown by means of the subscripts in these equations. The successful solution to this problem necessarily involves consideration of the over-all solution sequence. Figure 6a shows the general space-time representation of the solution. (An additional 3rd dimension exists at each point in the plate thickness direction. For the sake of simplicity, this dimension was not included in the figure.) In this figure, the steady state nodes at τ_o are known, since F0020 calculates from an initial steady state condition. Also, the tests were designed so that at the inlet, j=1, the quantities h_{il} and w_{il} would be known for all times. In the plate, the quantity q'''_{ijk} can be found from Eqs (27) and (28) for all times. Examination of Eqs (2)-(4) shows (1) the interaction of the plate on the fluid enters only through the flux (ϕ) in the enthalpy equation (2), and (2) the continuity equation (3) determines the local instantaneous flow at any axial location if the local fluid thermal conditions are known. The important corollary of this fact is that for the flow-forcing model of F0020, the pressure drop equation can be calculated after the thermal situation is known. Further, the thermal calculation is independent of the pressure drop equation (4).

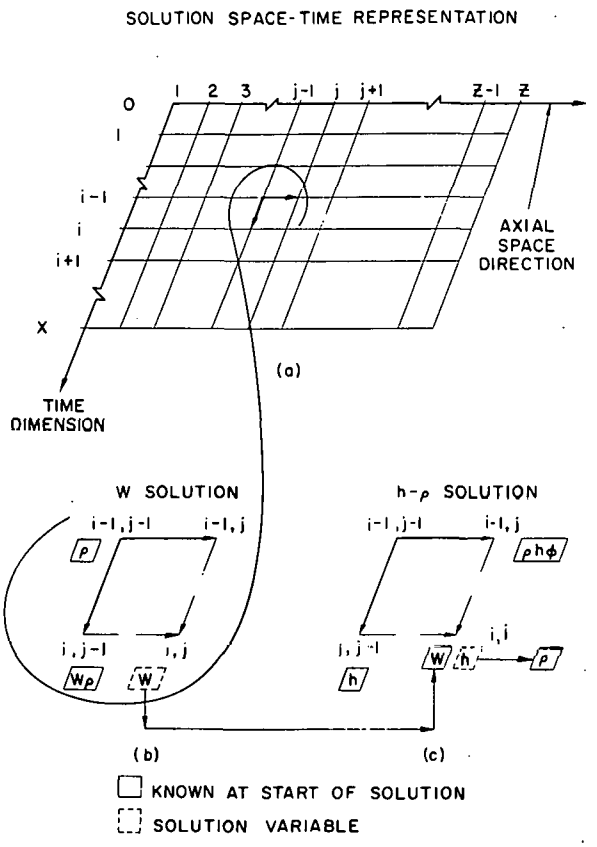

Fig. 6 Fluid Node Solution Sequence

As a result of the above considerations, the following solution method was used. The solution uses known conditions at previous time and space increments, as shown in Fig. 6a. To demonstrate the method, consider the fluid equations (17)-(23). The solution will proceed as follows:

1) At the ij^{th} position, where the solution is known at all j's at the i-1 time and at all times through i at the j-1 position, the solution can proceed as shown in Figs. 6b and 6c. (Such a position initially exists at node 1, 2 of Fig. 6a.) The continuity equation (18) allows solution for W_{ij} as shown in Fig. 6b. Then the enthalpy equation (17) can be used for finding h_{ij} as shown in Fig. 6c. ρ_{ij} is then calculated from Eq (62) or Eq (63).

2) The solution can then sequentially progress to either the i, j+1 node or the i+1, j node. Because the Bettis uniform axial generation test involves the most adverse thermal situation at the channel outlet, the former sequence was chosen; i.e., proceeding down the channel at a constant time.

The fluid solution must now be tied to the plate solution. This procedure involves the compatibility of the calculational times for the two components.

The stability criterion for the plate has been taken as (Eq 16)

$$\frac{(\Delta x)^2}{\alpha \Delta \tau} \equiv 3 \ .$$

Thus, for a given test specimen, this $\Delta\tau$, designated as $\Delta\tau_{plate}$, is fixed to insure stability of the calculation in the plate.

The corresponding criterion for the fluid requires that a piece of fluid appearing at any node does not pass the next downstream node in the time interval considered. This means that the fluid whose properties are estimated at one node must not pass out of the spatial extrapolation range in the time considered. This is checked by the transport equation

$$\Delta\tau_{transport} = \Delta z' \, \rho_{i-1,z} \, A_F / W_{i-1,1} \ , \qquad (67)$$

where $\Delta z'$ is the smallest axial grid length, $\rho_{i-1,z}$ is the minimum density of the previous time interval, and $W_{i-1,1}$ is the inlet flow of the previous time. This gives a conservative (small) value of $\Delta\tau_{transport}$ for loss of flow accidents. The two times, $\Delta\tau_{plate}$ and $\Delta\tau_{transport}$, are then reconciled as follows:

1) The ratio $\dfrac{\Delta\tau_{plate}}{\Delta\tau_{transport}}$ is formed.

2) The value of this ratio is increased to the next highest integer, N'.

3) The fluid extrapolation time is then

$$\Delta\tau_{fluid} = \Delta\tau_{plate}/N' \ . \qquad (68)$$

The over-all solution sequence (refer to Fig. 7) is:

1) Starting at solution time i-1, where all quantities are known, the $\Delta\tau_{fluid}$ is found from Eq (67) and (68).

2) The fluid solution is extrapolated ahead in time a quantity $\Delta\tau_{fluid}$ and sequentially down the axial nodes to the end of the channel.

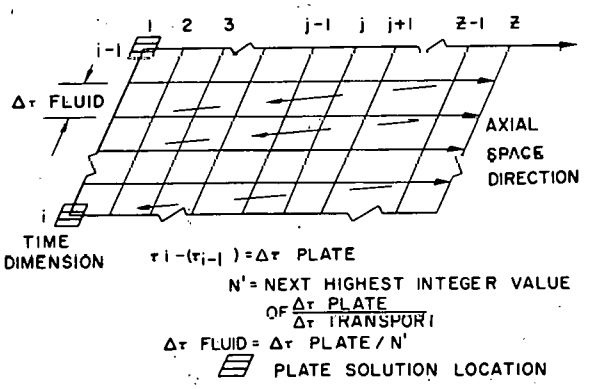

Fig. 7 Fluid Axial Solution Sequence

3) The solution then reverts to the inlet, and the extrapolation is made for another $\Delta\tau_{fluid}$ time. This process is repeated N' times until the fluid equations are solved to include the i^{th} time of Fig. 7. At this time, using the water properties at the i^{th} time, the plate equations are solved, starting at j_1 and proceeding to j_z.

4) At plate intervals, specified as input, the pressure drop equations (19)-(23) are solved. Since the thermal solution above is independent of the pressure drop solution, this pressure drop calculation is not a required part of the solution sequence.

Plate Surface Heat Flux Solution

The final solution sequence to be considered is that of application of the surface heat flux boundary condition (Fig. 5) to the plate conduction equations. The following solution sequences resulted in a satisfactory plate solution convergence for the particular test cases tried to date with F0020. In most cases, the methods were empirically derived by machine computation. The solution sequences are as follows. (As indicated in the section titled Over-All Fluid Plate Solution Sequence above, the water properties are already known at time i.)

1) Forced convection

Sequence	Calculated Variable	Eq No.
1	H_{ij}	(32)
2	T_{ijs}	(11)
3	T_{ijl}	(9)
4	$\overline{T}_{ij}$	(14)
5	ϕ_{ij}	(30)

2) Nucleate boiling

Sequence	Calculated Variable	Eq No.
1	T_{ijs}	(12)
2	T_{ijl}	(9)
3	$\overline{T}_{ij}$	(14)
4	ϕ_{ij}	(35)

3) DNB

Sequence	Calculated Variable	Eq No.
1	ϕ_{ij}	(36) or (37)
2	$\overline{T}_{ij}$	(15)
3	T_{ijl}	(10)
4	T_{ijs}	(13)

4) Partial film boiling

Sequence	Calculated Variable	Eq No.
1	ϕ_{ij}	(38)
2	$\overline{T}_{ij}$	(15)
3	T_{ijl}	(10)
4	T_{ijs}	(13)

5) Film boiling

Sequence	Calculated Variable	Eq No.
1	ϕ_{ij}	(39)
2	$\overline{T}_{ij}$	(15)
3	T_{ijl}	(10)
4	T_{ijs}	(13)

These sequences were found to produce the most stable perturbation responses for the plate surface as the solution transverses the boundary regions of Fig. 5. Equations (6)-(8) for the internal nodes are the same for all heat transfer regions.

MODEL LIMITATIONS

The following model limitations are cited for the consideration of the potential code user.

Heat Transfer Boundary Conditions

The principal limitation of the code is the uncertainty in describing the heat transfer boundary conditions of regions C, D, and E of Fig. 5. It is assumed that the transient ϕ_s plane is the same as the steady state plane. This is reflected in the code input in that the correlation constants for regions D and E, and the dividing temperature, T'_{crit}, are left as input. The height of region C may also be indirectly changed by the input DNB time.

Continuity Equation Instability

An instability in the local flow as calculated by the continuity equation (18) has been noted in some of the test cases. The cause of this instability has been traced to the combination of two factors. One is the Δz in the numerator of Eq (18) and the other is the discontinuity in the curve fit of ρ_{ij} vs h_{ij} at h_{sat} [Eq (60) and (61)]. This discontinuity in W_{ij} is shown in Fig. 8. The discontinuous point occurs when the point downstream passes into bulk boiling and the extrapolation length Δz is large in Eq (18). For a test case where Δz was 8 in., the increase in flow was approximately 10% at the surge points of Fig. 8. This oscillation occurred at all points downstream of a node, progressing into bulk boiling because of the W_{ij-1} term of Eq (18).

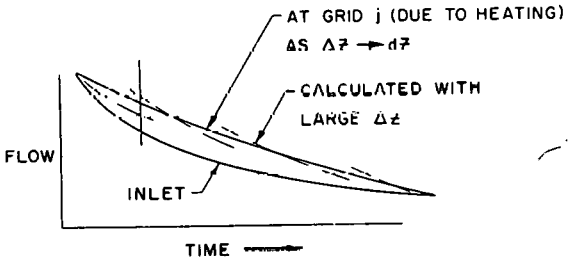

Fig. 8 Flow Oscillations (Calculated) Resulting from Large Grids and Break in ρ_z vs h_z Curve at h_{sat}

Mathematically, this effect is a result of allowing the expansion caused by bulk boiling to progress in finite steps of Δz length. The solution flow, as calculated with a grid length of Δz, oscillates around the true flow (as $\Delta z \to dz$), as shown in Fig. 8. While this oscillation will not greatly affect the local flux at DNB, a borderline DNB point may come back out of DNB on the time interval following this local increase in flow. Two methods are available to minimize this effect: smooth the ρ_{ij} vs h_{ij} curve in the h_{sat} region, or use smaller Δz values. While it is possible that the density variation at the inception of bulk boiling is more continuous during a transient than during steady state conditions, no data of transient ρ_{ij} vs h_{ij} are available. Therefore, it is recommended that smaller values of Δz be used. The recommended procedure is as follows:

1) Using initial flux values, flow coastdown information, and desired accident computation time, compute the length of the first grid necessary to cause bulk boiling to just begin at this grid at the end of the desired running time. The formula for this purpose is derived as

$$671.7 = h_{i1} + \frac{2a\delta\Delta z_2\, \phi_{i2}}{W_{o2}\left[\frac{1}{1 + b\tau'}\right]} \tag{69}$$

from steady state considerations. In this equation $\phi_{i2} \approx \phi_{o2}\,[\bar{I}_i/\bar{I}_o]$ since local boiling will exist at point 2 prior to bulk boiling, and the plate temperature profile will approximate a steady state profile.

2) Using this value of Δz_2 for the length to the first grid, divide the remaining channel length into as many as 2 regions and 48 nodes.

Stability Checkout Limitation

The final limitation is concerned with the stability of the solution at all positions of the ϕ plane in Fig. 5. This stability has been found satisfactory for the test cases of loss of pumping power accidents. This stability has not been demonstrated for other types of accidents which may be suggested by the input format, such as rod withdrawal, etc.

CODING DETAILS

Code Description

The problem, as previously defined, was coded for the IBM-704 computer in the Fortran language with options of obtaining some of the variables plotted on the peripheral printer and of changing the heat generation function at a specified time during the problem (refer to Fig. 9 for flow diagram). The code is comprised of the following parts.

Initialization

The title card is read and printed on-line and written on tape. All data cards for the problem are read and checked against code limitations (set forth in a later subsection). If an error is detected it is printed on-line with instructions on how to continue. All of the computed equation coefficients and the plate time interval are calculated. The initial heat flux into the fluid and all fluid properties are calculated at all axial points by using the input forcing functions at zero time and the steady state form of the fluid equations. The metal surface temperatures are computed for all axial points, using Eq (11) or (12) with the restriction that T_{ijs} cannot exceed T_{scrit} (no DNB initially).

The internal finite difference plate temperatures are obtained by an iterative process after first computing an initial approximation from the one-dimensional analytic solution. This approximation is obtained by considering the plate to be composed, in general, of a heat generating material between non-generating materials. The limits of the generating material are determined from the input. For all radial points falling in the non-generating region nearest to the coolant, the initial temperature distribution is approximated from the equation

$$T(x) = q''' \frac{(\ell_a - \ell_b)x}{k} + T_s \quad . \tag{70}$$

For those points within the generating material region,

$$T(x) = \frac{q'''}{k} \left(\ell_a x - \frac{x^2}{2} - \frac{\ell_b^2}{2} \right) + T_s \quad . \tag{71}$$

Values of T on the adiabatic surface side of the generating material are constant and are obtained from Eq (71) by setting $x = \ell_a$. Using these initial approximations, the initial finite difference internal plate temperatures are obtained by iterating Eqs (6)-(9) to a convergence, ϵ, specified in the input. This method has been found satisfactory for problems with and without non-generating regions.

All of the initial values are written on the computer storage tape and, if plotting has been requested, the initial values of water temperature, metal surface temperature, thermocouple temperature, and flux for all axial points are saved in the computer storage core.

Water Calculation

The fluid equations for all axial points are advanced by time steps until a time has been reached for evaluation of the plate properties. The time interval used for the fluid equations is determined by selecting the first submultiple of the plate time that is equal to, or less than, the fluid transport time across the smallest axial mesh distance. The fluid properties are calculated, using the forcing function equations (24) and (25) and fluid equations (17) and (18) and (58) through (63) (refer to Fig. 10).

Plate Calculation

The method of calculating the plate properties at a given point depends on the history of the point. The flow diagram is shown in Fig. 11. In all cases, the internal plate temperatures and T_{ijw} are first calculated, using Eqs (6), (7), (8), and (58) or (59). There are two possible paths from this point:

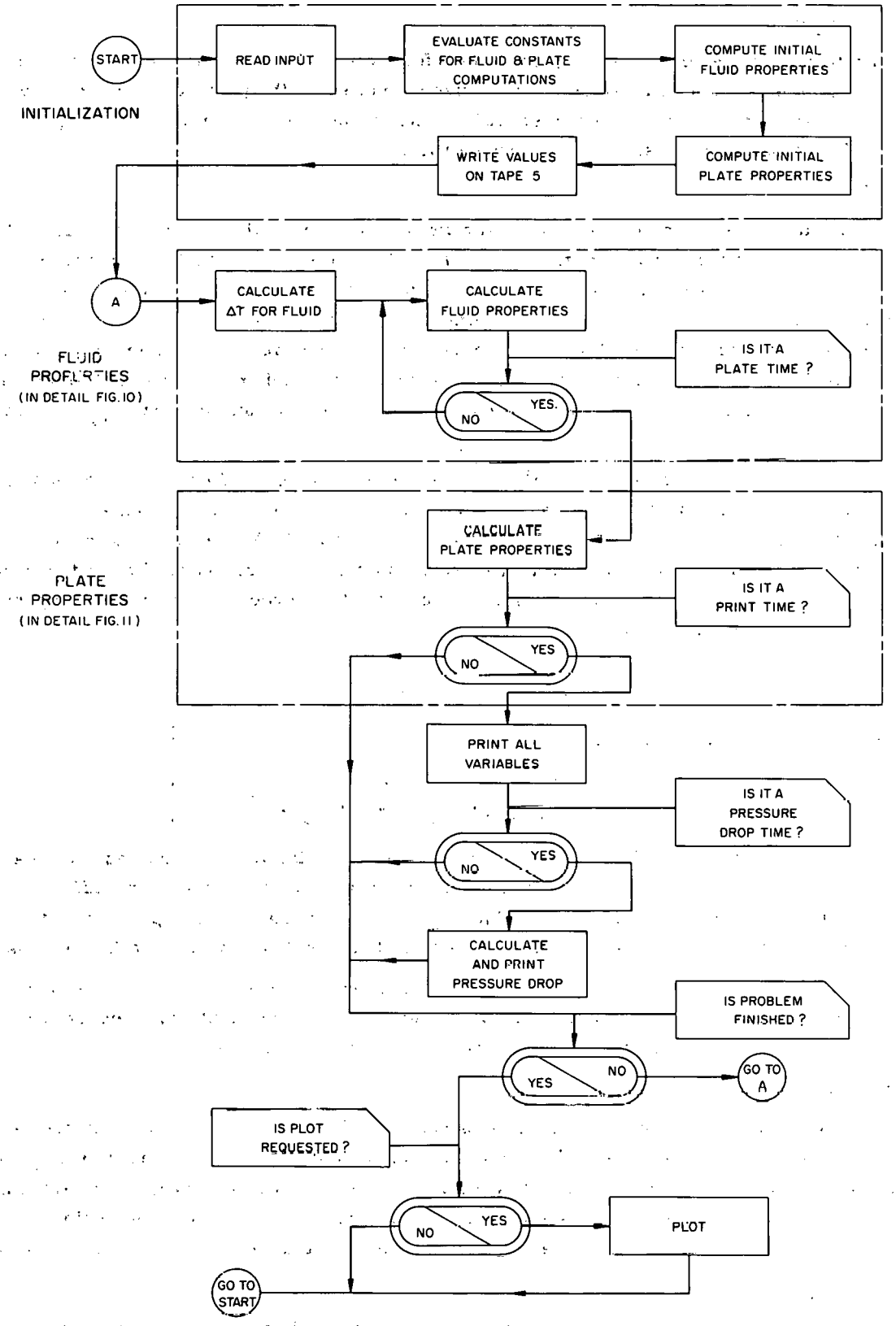

Fig. 9 General Flow Diagram

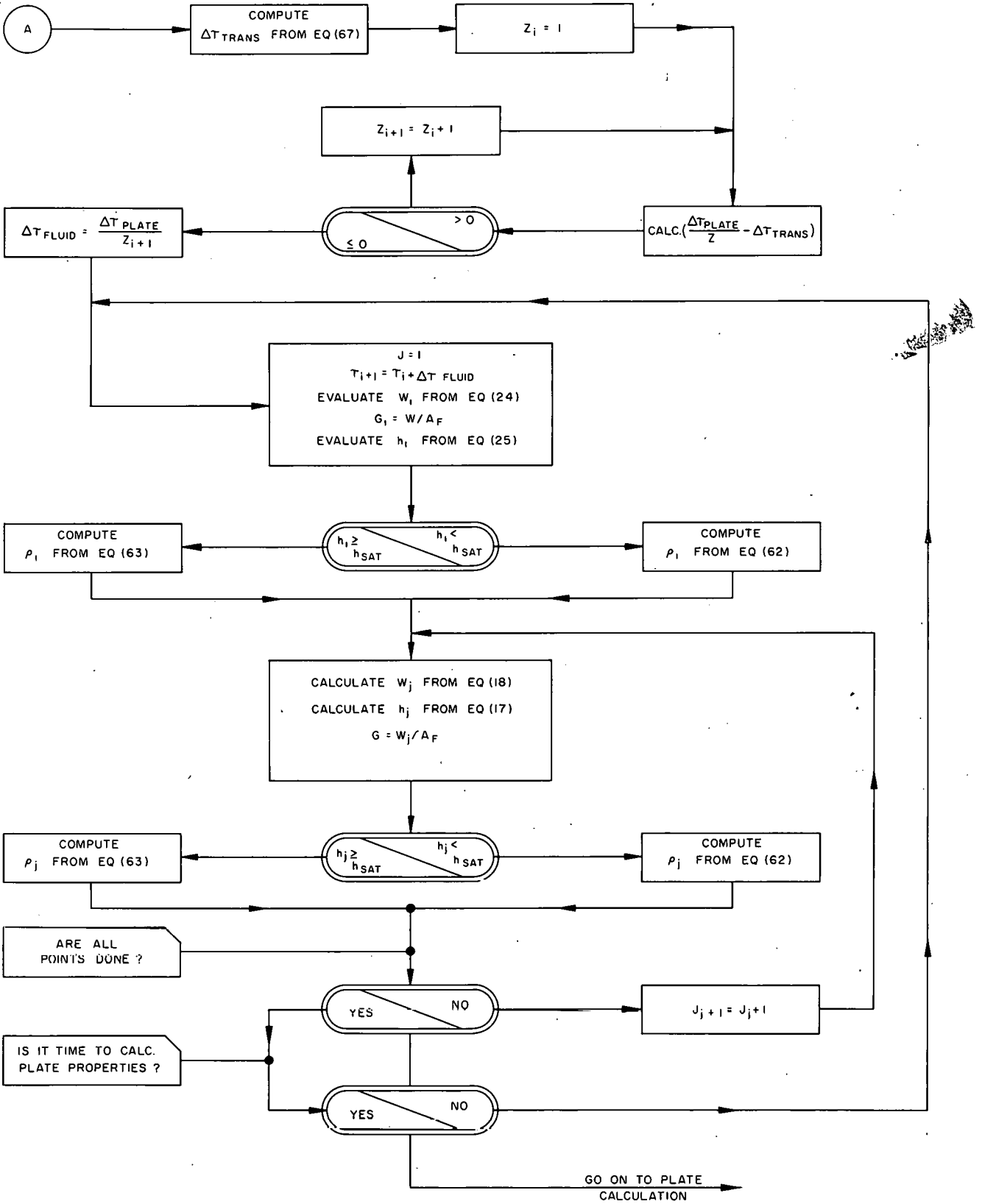

Fig. 10 Fluid Property Diagram

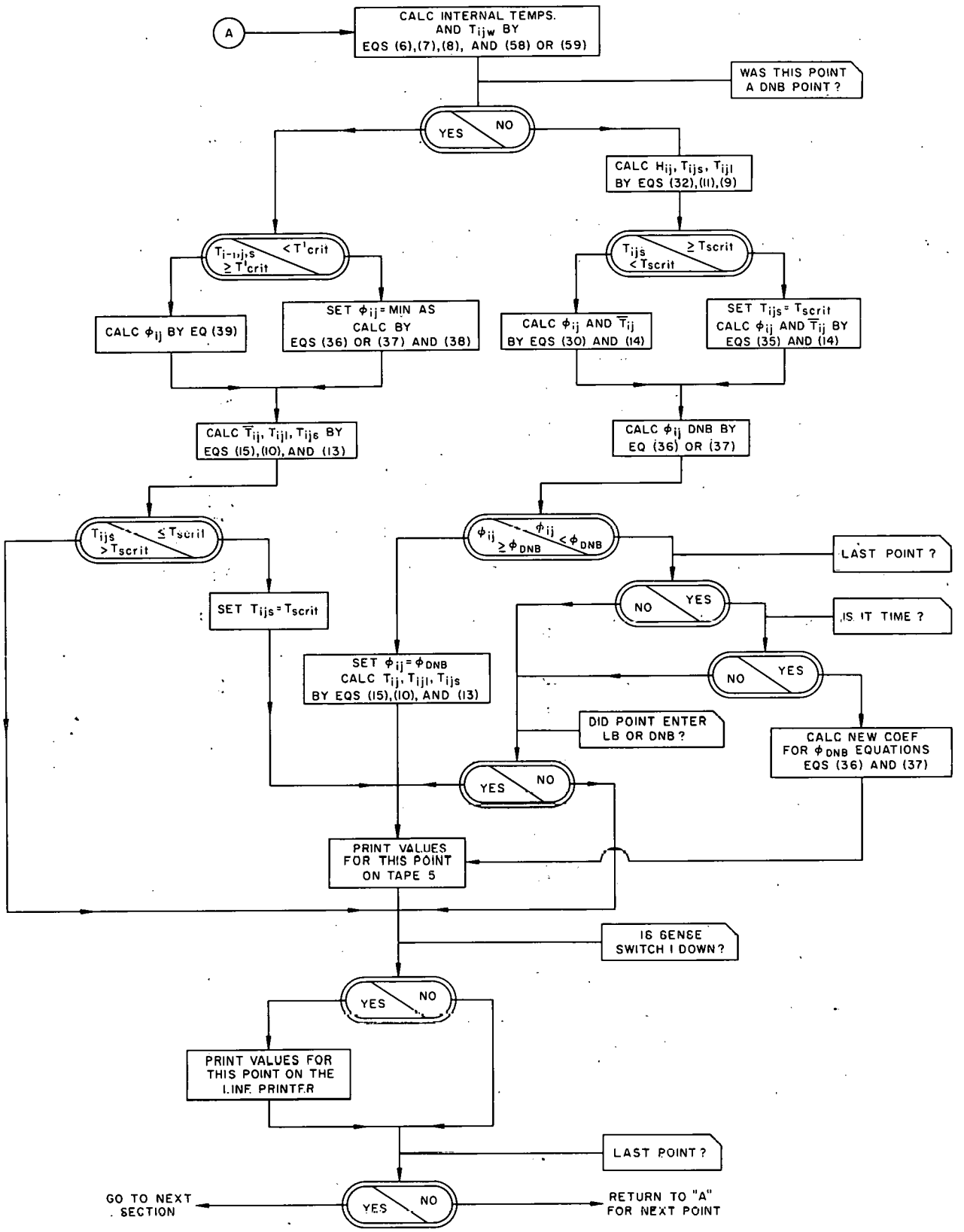

Fig. 11 Fluid Property Diagram

1) If the point was in forced convection or local boiling for the last time step, T_{ijl}, T_{ijs}, and H_{ij} are evaluated, using Eqs (9), (11), and (32). Then T_{ijs} is checked as follows to allow solution reversibility between force convection and nucleate boiling:

   a) If $T_{ijs} < T_{scrit}$, the flux and average plate temperature are evaluated, using Eqs (30) and (14).

   b) If $T_{ijs} \geq T_{scrit}$, T_{ijs} is set equal to T_{scrit}, and the flux and average plate temperature are calculated, using Eqs (35) and (14).

   In either case, the flux is next compared with a DNB flux as evaluated from Eqs (36) or (37). If $\phi_{ij} < \phi_{DNB}$, then the computation for the point is completed. If $\phi_{ij} \geq \phi_{DNB}$, ϕ_{ij} is set equal to ϕ_{DNB}, and $\overline{T}$, T_{ijl}, and T_{ijs} are evaluated from Eqs (15), (10), and (13). The computation for the point is then complete. The indicator in (1) above is set to DNB.

2) If, at the last time step, the point was not forced convection or nucleate boiling, the surface temperature is checked.

   a) If film boiling does not exist ($T_{i-1,js} < T'_{crit}$), the flux is set equal to the minimum flux from Eqs (36) or (37) and (38). The newly calculated T_{ijs} is now checked as follows. If $T_{ijs} < T_{scrit}$, it is set equal to T_{scrit} and the indicator checked in (1) above is set to local boiling for the point. This check allows solution reversibility between nucleate boiling and DNB or partial film boiling.

   b) If film boiling exists ($T_{i-1,js} \geq T_{crit}$), the flux is evaluated from Eq (39).

   In either case, $\overline{T}_{ij}$, T_{ijl}, and T_{ijs} are then calculated, using Eqs (15), (10), and (13).

   When a point enters either the nucleate boiling or the DNB region, all variables at that point are written on tape. It is also possible to force the last point to DNB at a time specified in the input. If DNB has not previously occurred at the last point at the specified time, the coefficients for Eqs (36) and (37) are recalculated to set $\phi_{iz} \equiv \phi_{ij}$ in these equations.

Output*

The output parameters are written on magnetic tape for printing on the peripheral printer. The desired frequency of output is an input parameter. At an output time, the pertinent parameters for all axial points are written on tape, and, if plotting has been requested, T_{ijw}, T_{ijs}, T_{ijTC}, and ϕ_{ij} are saved in the computer core.

Pressure Drop Calculation

The frequency of pressure drop calculation is an input parameter. These results, written on tape, indicate the contributions of elevation, space acceleration, time acceleration, and friction as well as the total pressure drop. These results are calculated for three regions: from the inlet to the first point after the inlet, and from the inlet to the next to the last and to the last point. The method of calculation is indicated by Eqs (40)-(55). If plotting has been requested, the total pressure drop and inlet flow are saved in the computer core.

Plot

If plotting has been requested, the variables saved in the computer core are checked to find the maximum thermocouple temperature, minimum water temperature, maximum and minimum of flux, total over-all pressure drop, and inlet flow for the problem. Each plot point is then normalized to the maximum-minimum problem range, so that all curves will be scaled from 0 to 1. All temperatures are plotted on the same scale. The values of time associated with the variables are also

* The output is described in the section titled Sample Problem.

normalized, so that the accident time is scaled from 0 to 1.

The following plots are then prepared:

1) One plot of total pressure drop, from inlet to exit, and inlet flow versus time.

2) One plot for each axial point of water temperature, surface temperature, thermocouple temperature, and flux versus time.

The plots are formed on the peripheral printer with the grid lines indicated by plus (+) signs and the plotted variables by letters which are identified on each page. In addition, the problem title, scaling, and point number appear with each graph. Each graph is 100-type wheels across the paper and 100-lines long. The graphs extend across two pages and are approximately 10 in. x 16 in. in size.

Input

Input Information

The following information must be supplied to define a F0020 problem. The input contains integer and non-integer quantities. (For the definition of integer and non-integer quantities, see the following section.) A sample input is shown in Fig. 12.

1) Title card:
   a) Columns 2-67 are available for the title.
   b) Columns 68-71 must contain F0020.
   c) Column 72 is used to denote a particular version of the code. This version is 0 (zero).

2) Card 1001:
   a) Accident time in seconds
   b) Print frequency in seconds

      (NOTE: The actual frequency of output will not be exactly this value since the elapsed time is compared with this input, and printing occurs when elapsed time exceeds multiples of the input print frequency.)

   c) DNB time in seconds. (DNB occurs when elapsed time exceeds this input.)
   d) Pressure drop frequency (integer). This is the number of normal print-outs per pressure drop calculation.
   e) X (integer). If X = 1, the radial heat generation is uniform. If X = 0, the heat generation is specified pointwise on card 1010.
   f) Z (integer). If Z = 1, the axial heat generation is uniform. If zero, the values must be specified, starting on card 1011 at 10 values per card.
   g) IP (integer). If IP = 1, plotting is requested. If IP = 0, plotting is not requested.

3) Card 1002:
   a) Water channel thickness
   b) Water channel width
   c) Plate thickness
   d) Plate width
   e) Time, in seconds, to change I forcing function; if 0, no change will be made.

TITLE CARD

	SAMPLE PROBLEM FOR WAPD-TM-145 - July 7, 1958 F0020

	ACC. TIME	PRINT TIME	DNB TIME	NPPPD	X	Z	IP
1001	2.31480000	.04629600	.500000000	1	1	1	1

	CHAN. THK.	CHAN. WIDTH	PLATE THK.	PLATE WIDTH	I CHANGE		
1002	.008333333	.083333333	.004166667	.070000000	0.000000000		

	W_o	LIN. COEF.					
1003	1500.00000	2.000000000					

	h_o	LIN. COEF.					
1004	320.000000	0.000000000					

	I_o	LIN. COEF.	SQ COEF.	MP/4	ALT. LIN. COEF.	ALT. SQ. COEF.	
1005	2700.00000	0.000000000	0.000000000	.000028188	0.000000000	0.000000000	

	D_e	T_w SAT					
1006	.015151515	635.78000					

	A	B	C	D	a		
1007	26400000.00	2000.00000	-1585000.0	12500.000	1.050000000		

	K	ρ_M	C_p	T_s CRIT.	T' CRIT.	ϵ	
1008	12.000000000	500.000000	.120000000	641.50000	1300.00000	.010000000	

	#ΔX	#REG	ΔZ_1	P_1	ΔZ_2	P_2	ΔZ_3	P_3	
1009	3	1	.166666667	9					

(CARD 1010 IS USED ONLY IF X IS ZERO)

	NX_1	NX_2	NX_3	NX_4	NX_5	NX_6	NX_7	NX_8	NX_9	NX_{10}	
1010											

(CARD 1011 IS USED ONLY IF Z IS ZERO)

	NZ_1	NZ_2	NZ_3	NZ_4	NZ_5	NZ_6	NZ_7	NZ_8	NZ_9	NZ_{10}	
1011											

Fig. 12 Input for Sample Problem

4) Card 1003:

   a) W_o. Initial flow (W_{o1})

   b) Flow decay coefficient (b) in Eq (24)

5) Card 1004:

   a) h_o. Initial enthalpy (h_{o1})

   b) Enthalpy coefficient (c) in Eq (25)

6) Card 1005:

   a) I_o. Initial average current ($\bar{I}_o$)

   b) Linear coefficient (d) for current in Eq (26)

   c) Second degree coefficient (e) for current in Eq (26)

   d) Conversion factor $M\rho_{E/4}$ in Eq (27)

   e) Alternate values of (2) [only if (5) on card 1002 $\neq 0$]

   f) Alternate values of (3) [only if (5) on card 1002 $\neq 0$]

7) Card 1006:

   a) Hydraulic diameter

   b) Coolant saturation temperature

8) Card 1007:

   a) A, B, C, and D in flux Eqs (38) and (39)

   b) Heat pickup correlation term "a" in Eq (17)

9) Card 1008:

   a) K = Plate thermal conductivity

   b) ρ_M = Density of plate

   c) C_p = Specific heat of plate

   d) $\bar{T}_{scrit}$ - Temperature of plate surface at which nucleate boiling begins

   e) T'_{crit} = Temperature of plate surface at which transition from partial film boiling to film boiling occurs

   f) ϵ = Convergence criterion, in degrees F, for iteration of plate temperatures to their initial finite difference values

10) Card 1009:

   a) #Δx = Number of radial sections in plate (integer)

   b) #Reg = Number of axial regions (integer)

   c) Δz_i = Mesh length in axial region i

   d) P_i = Axial point to which region i extends (integer)

11) Card 1010:

   a) NX_i = Radial generation factor, $\bar{F}_K$, at plate radial node k (Specify a value for each node.)

12) Cards 1011, 1012.....etc:

   a) NZ_i = Axial generation factor, F_j, at plate position j (Specify a value for each axial point; ten values per card.) Used only if Z = 0 on card 1001.

Definition of Integer and Non-Integer Input

1) Integer: Numbers with no decimal point specified, such as 1

   (NOTE: Integers on the input form, must be moved to the far right of the specified field. Example: Let #Δx on card 1009 be 3. The field is 5 columns wide. Place the number 3 in rightmost column of the field, which would be card column 10 in this case. If the number 3 were placed in card column 9, it would be interpreted as 30.)

2) Non-integer: Numbers with the decimal point indicated, such as 1.0. An example of this representation of the number 0.00127 would be any of the following:

   0.00127
   0.127E-2
   127.E-5

   This type of input may be positioned anywhere within the number field. A blank column is interpreted as a zero.

Code Limitations

The following limitations must be observed by code users:

1) Total number axial regions: $1 \leq \#Reg \leq 3$.

2) Total number of axial points (including inlet point): ≤ 50.

3) Total number of radial regions: $3 \leq N \leq 10$.

4) DNB time < accident time (accident calculations must include a DNB).

5) If plotting is requested:

$$\frac{\text{accident time}}{\text{print frequency}} < 50$$

   (Because plot time is normalized, the requestor may want to choose an accident time to permit easy reference to the plots.)

6) All input floating numbers are rounded to eight places.

Running Time

The machine time required for a time step depends on the number of axial and radial points. The number of time steps depends on the specified accident time and the computed time interval for the plate properties. The time interval used in the fluid calculation depends on the plate time interval and the fluid transport time, which varies during a problem. It is, therefore, possible to give only a sample running time.

For the sample problem of this report, the 704 running time was 3.3 minutes for the calculation and normal print-out, plus 50 seconds for the plots.

Of the 3.3 minutes of running time, approximately 1.5 minutes were used in writing the output on tape.

Machine Requirements

The code requires the following machine components:

1) Core size—32 k

2) Number of tapes—2

3) On-line card reader

4) On-line printer (SHARE-2 printer board)

5) Off-line printer

The off-line printer must not have the modification to restore at the end of a page when operating under program control. This permits the plots to extend over two pages without a discontinuity.

Operating Instructions

Code running proceeds as follows:

Write Program Tape

1) Set a tape to logical 1.

2) Ready the card program in reader.

3) Press "clear" button, then "load card" button. [Stops at $(343)_8$ after rewind of tape 1.]

Running the Problem

1) Mount on tape unit 1 the program tape written as above.

2) Make ready a blank tape on unit 5.

3) Ready the data input in the card reader.

4) Place SHARE-2 printer board in printer.

5) Place all Sense Switches on console in "up" position.

6) Press "clear" button, then "load card" button.

Stops*

1) 11111—more than 50 axial points

2) 20000—normalization error in input

3) 70707 read comment on-line

4) 10000—probable machine error

5) 20202 probable machine error

6) 30000 probable machine error

7) 00010—probable machine error

8) 00030—probable machine error

9) Normal end of problem—select on card reader. (Print tape 5 on program control.)

SAMPLE PROBLEM

The following problem illustrates typical code usage.

Problem Specification

Consider the thermal and hydraulic response of a plate-channel element with constant uniform internal heat generation, constant channel inlet enthalpy, and an imposed flow coastdown. (All input data for this problem is given on the sample input form, Fig. 12.) The initial problem conditions were selected such that the solution would traverse all regions of the heat transfer boundary condition representation (Fig. 5) in a reasonable running time. The channel length was broken into eight equal lengths for a total of nine axial (j) nodes, including the inlet, j1. The plate thickness was

* The octal numbers will be in the address of the storage register.

broken into three equal radial regions and associated nodes. A DNB time of 0.50 sec was selected to insure proper problem T_{TC} coverage.

Digital Output

Figure 13 shows the following code digital print-out. All digital output is in the form 0.xxxx ± Eyy; which means the digital number is equal to (±0.xxxx) multiplied by $(10)^{\pm yy}$.

Regular Output

The large central block of information in Fig. 13 is an example of the regular print-out which occurs at the desired print integral. After the identifying time, the following information is given for each node:

1) Line 1:
   a) Column 1—axial (j) node number
   b) Column 2—flow
   c) Column 3—enthalpy
   d) Column 4—density
   e) Column 5—forced convection film coefficient (only recomputed if solution is in region A or B of Fig. 5—otherwise, this is last computed value)
   f) Column 6—water temperature
   g) Column 7—surface heat flux
   h) Column 8—plate surface temperature
   i) Column 9—plate thermocouple temperature
2) Line 2:
   a) Column 1—plate radial (k) node 1 temperature
   b) Column 2—plate radial (k) node 2 temperature
   c) Column 3—plate radial (k) node 3 temperature
   d) Column 4—plate radial (k) node 4 temperature
   e) Column 5—plate radial (k) node 5 temperature
   f) Column 6—plate radial (k) node 6 temperature
   g) Column 7—plate radial (k) node 7 temperature
   h) Column 8—plate radial (k) node 8 temperature
   i) Column 9—plate radial (k) node 9 temperature
   j) Column 10—plate radial (k) node 10 temperature

(unused nodes are left blank on print-out)

Special Print-Outs

Two special print-outs are also shown in Fig. 13 as follows:

Special Heat Transfer Mechanism Change—The top of the figure shows the special print-out of the individual node (same information as regular print-out) that occurs when any node progresses into, or departs from, the nucleate boiling region. (In the example, point 5 has progressed into the DNB region (C) of Fig. 5 at 1.447 sec.) This information is given for the iteration cycle within which the event occurred, even if this cycle is not a regular print-out cycle.

TIME =0.1447E 01 SECONDS

J	FLOW	ENTHALPY	DENSITY	H	TW	FLUX	TS	TTC
5	0.3887E 03	0.5585E 03	0.4606E 02	0.2127E 04	0.5582E 03	0.1004E 07	0.6416E 03	0.8210E 03

T1	T2	T3	T4	T5	T6	T7	T8	T9	T10
0.700E 03	0.777E 03	0.816E 03							

SAMPLE PROBLEM FOR WAPD-TM-145 - JULY 7, 1958 F0020

TIME =0.1481E 01 SECONDS

J	FLOW	ENTHALPY	DENSITY	H	TW	FLUX	TS	TTC
1	0.3785E 03	0.3200E 03	0.5607E 02	0.1735E 04	0.3396E 03	0.1006E 07	0.6415E 03	0.8210E 03

T1	T2	T3	T4	T5	T6	T7	T8	T9	T10
0.700E 03	0.777E 03	0.816E 03							

J	FLOW	ENTHALPY	DENSITY	H	TW	FLUX	TS	TTC
2	0.3785E 03	0.3832E 03	0.5397E 02	0.1865E 04	0.4042E 03	0.1006E 07	0.6415E 03	0.8210E 03

T1	T2	T3	T4	T5	T6	T7	T8	T9	T10
0.700E 03	0.777E 03	0.816E 03							

J	FLOW	ENTHALPY	DENSITY	H	TW	FLUX	TS	TTC
3	0.3790E 03	0.4447E 03	0.5157E 02	0.1966E 04	0.4624E 03	0.1006E 07	0.6415E 03	0.8210E 03

T1	T2	T3	T4	T5	T6	T7	T8	T9	T10
0.700E 03	0.777E 03	0.816E 03							

J	FLOW	ENTHALPY	DENSITY	H	TW	FLUX	TS	TTC
4	0.3801E 03	0.5045E 03	0.4885E 02	0.2044E 04	0.5147E 03	0.1006E 07	0.6415E 03	0.8210E 03

T1	T2	T3	T4	T5	T6	T7	T8	T9	T10
0.700E 03	0.777E 03	0.816E 03							

J	FLOW	ENTHALPY	DENSITY	H	TW	FLUX	TS	TTC
5	0.3820E 03	0.5627E 03	0.4583E 02	0.2127E 04	0.5614E 03	0.9858E 06	0.6429E 03	0.8211E 03

T1	T2	T3	T4	T5	T6	T7	T8	T9	T10
0.701E 03	0.778E 03	0.816E 03							

J	FLOW	ENTHALPY	DENSITY	H	TW	FLUX	TS	TTC
6	0.3847E 03	0.6131E 03	0.4292E 02	0.2551E 04	0.5937E 03	0.7747E 06	0.7175E 03	0.8714E 03

T1	T2	T3	T4	T5	T6	T7	T8	T9	T10
0.776E 03	0.836E 03	0.869E 03							

J	FLOW	ENTHALPY	DENSITY	H	TW	FLUX	TS	TTC
7	0.3879E 03	0.6525E 03	0.4045E 02	0.2911E 04	0.6257E 03	0.6457E 06	0.8256E 03	0.9642E 03

T1	T2	T3	T4	T5	T6	T7	T8	T9	T10
0.884E 03	0.934E 03	0.959E 03							

J	FLOW	ENTHALPY	DENSITY	H	TW	FLUX	TS	TTC
8	0.3914E 03	0.6854E 03	0.3279E 02	0.3239E 04	0.6358E 03	0.5561E 06	0.9324E 03	0.1061E 04

T1	T2	T3	T4	T5	T6	T7	T8	T9	T10
0.991E 03	0.103E 04	0.106E 04							

J	FLOW	ENTHALPY	DENSITY	H	TW	FLUX	TS	TTC
9	0.4135E 03	0.7130E 03	0.2491E 02	0.3606E 04	0.6358E 03	0.4908E 06	0.1033E 04	0.1154E 04

T1	T2	T3	T4	T5	T6	T7	T8	T9	T10
0.109E 04	0.113E 04	0.115E 04							

SAMPLE PROBLEM FOR WAPD-TM-145 - JULY 7, 1958 F0020

PRESSURE DROP CALCULATION AT T =0.1481E 01 SECONDS .

J	FRICTION	T - ACC	S=ACC	ELEVATION	TOTAL
1	0.1477E-01	-0.2765E-02	0.3350E-02	0.6365E-01	0.7901E-01
8	0.1494E-00	-0.1964E-01	0.7310E-01	0.3796E-00	0.5824E 00
9	0.1902E-00	-0.2315E-01	0.1487E-00	0.4130E-00	0.7288E 00

Fig. 13 Digital Output for Sample Problem

Special Pressure Drop Calculation—A special pressure drop calculation and associated print-out are performed when specified in the input. (For the sample problem, a pressure drop calculation was performed for each thermal calculation.) The pressure drop print-out is shown at the bottom of Fig. 13. The individual pressure drop components and the total pressure drop are listed for the following axial points:

1) Inlet to second node (designated as j1 in ΔP print-out)
2) Inlet to next to the last node (j8 for sample problem)
3) Inlet to last node (j9 for sample problem)

Calculations (1) and (2) above allow interpolation in the event that the axial calculation grid cannot be aligned with the test specimen pressure taps.

The column identification for this special print-out is as follows:

1) Column 1—downstream node to which ΔP is calculated (except first line in which j1 designates inlet to second node).
2) Column 2—frictional component [Eq (19)]
3) Column 3—time acceleration component [Eq (20)]
4) Column 4—spatial acceleration component [Eq (21)]
5) Column 5—elevation component [Eq (22)]
6) Column 6—total pressure drop [Eq (23)]

Plot Output

At the option of the problem requestor, the code will plot, in normalized form, the following regular digital print-out information:

ΔP_{Total} and W_{i1} versus τ (1 plot only)

Figure 14 shows the code plot of over-all total pressure drop and inlet flow versus accident time for the sample problem. (Scaling numbers are in direct digital form.)

T_{ijw}, T_{ijs}, T_{ijTC}, and ϕ_{ij} versus τ (1 plot at each j node)

Figure 15 shows the code plot of water temperature, surface temperature, thermocouple temperature, and surface heat flux versus accident time at point 8 (axial node 8) of the sample problem. (Scaling numbers are in direct digital form.)

Sample Problem Analysis

Several items shown on Figs. 14 and 15 are of interest in the sample problem.

Figure 14

The inlet flow for the sample problem is shown in Curve A of Fig. 14. The pressure drop is shown in Curve B. At approximately 0.53 of the normalized time scale, a pressure increase is shown. This increase is caused by coolant expansion (steam formation) in the channel causing the increase in the spatial acceleration component to become larger than the decrease in the frictional and elevation pressure components.

Figure 15

Figure 15 shows the pertinent heat transfer parameters for grid 8. (Grid 8 is 14 in. from inlet in sample problem.) This grid was chosen as an example because it experiences all methods of heat transfer depicted in Fig. 5.

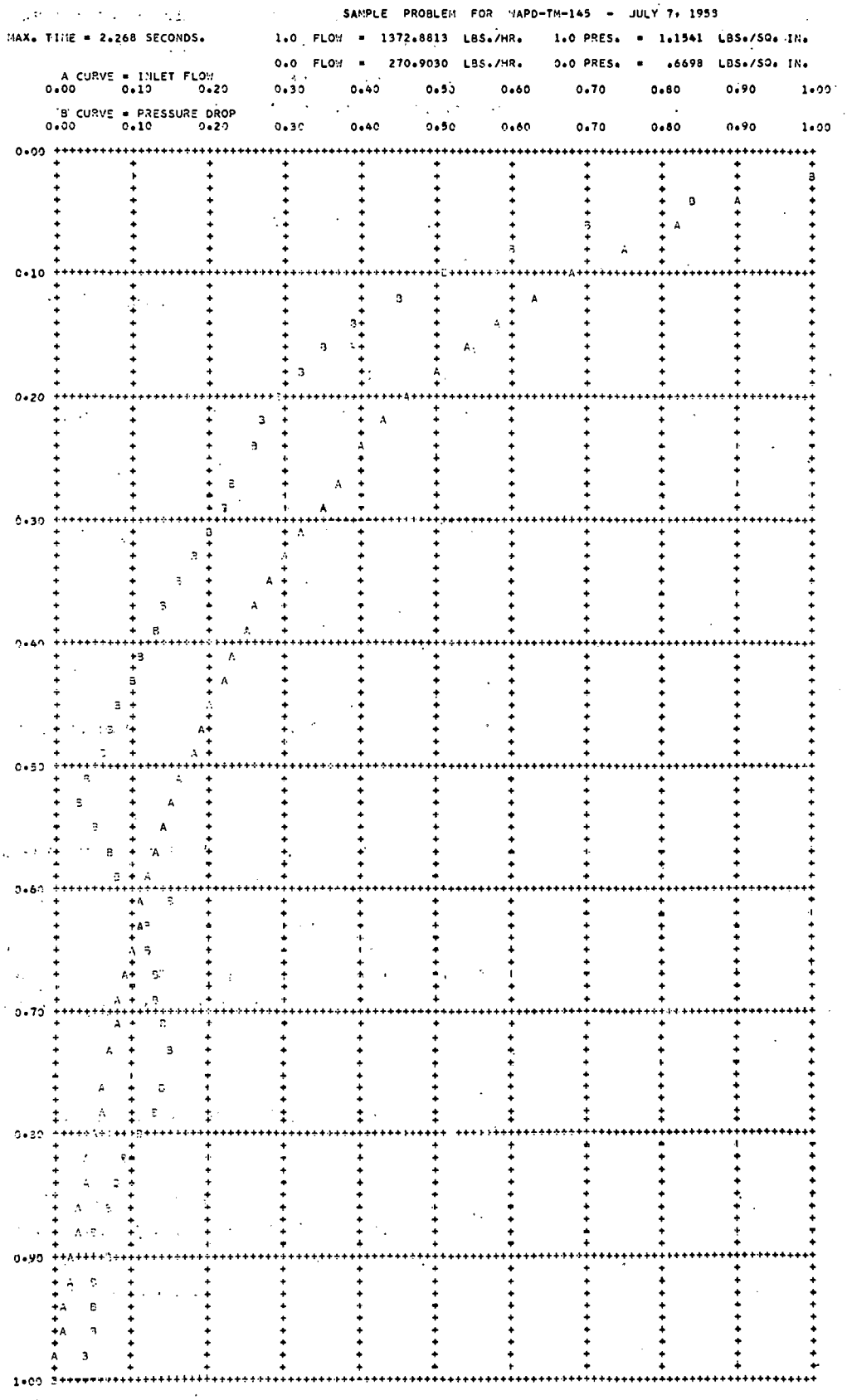

Fig. 14 Plot of Pressure Drop and Inlet Flow vs Time for Sample Problem

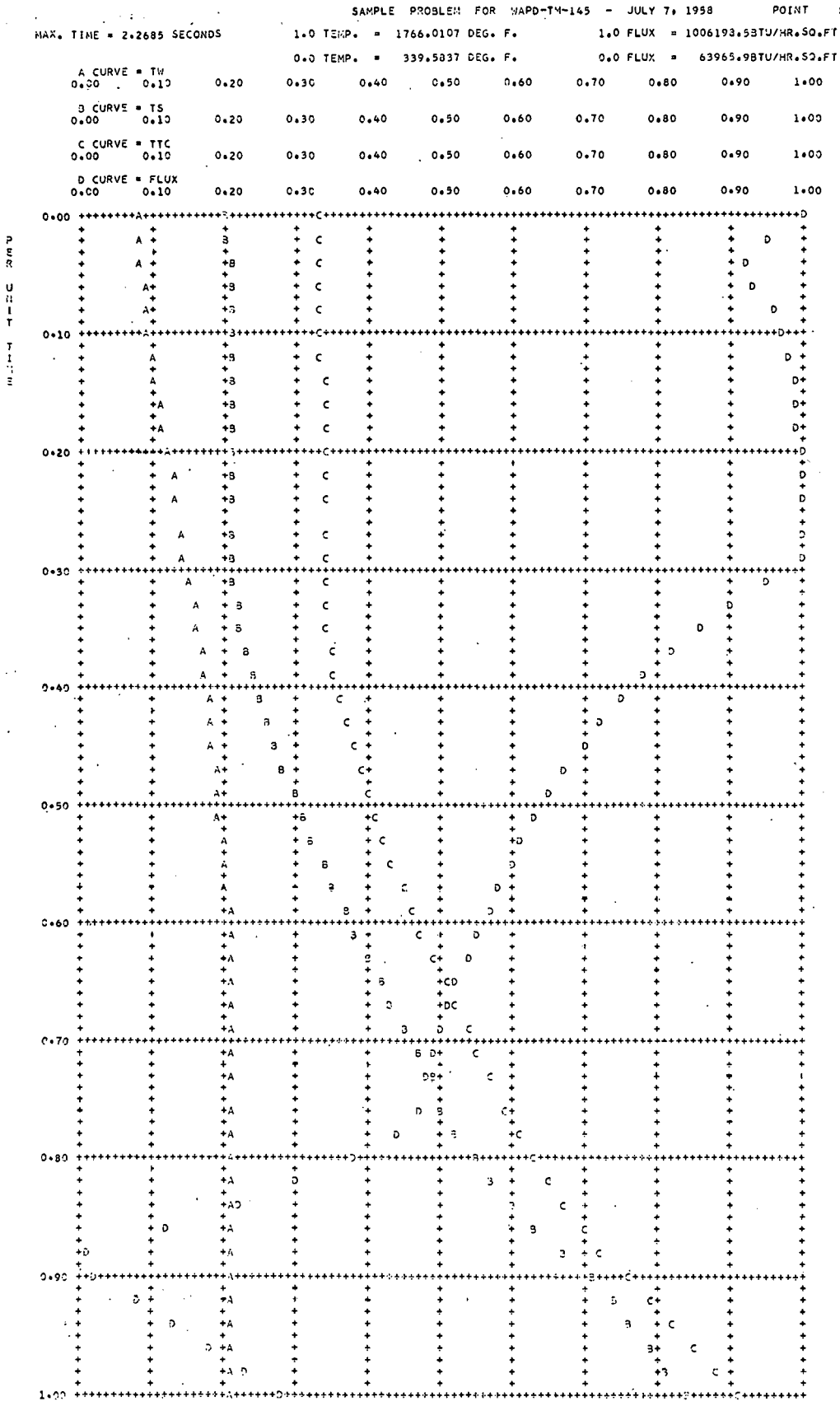

Fig. 15 Plot of Water Temperature, Thermocouple Temperature, Surface Temperature, and Surface Flux vs Time for Sample Problem

Examination of Fig. 15 shows the following relationships between time and heat-transfer mechanism:

Normalized Time	Type of Heat Transfer	Region (Fig. 5)
0.00-0.05	Forced convection	A
0.05-0.29	Nucleate boiling	B
0.29-0.76	DNB	C
0.76-0.88	Partial film boiling	D
0.88-1.00	Film boiling	E

Constant heat generation was purposely specified to illustrate the transient flux effect. For the example problem, the steady state flux is equivalent to the 1.00 normalized flux line. The difference between this line and the transient flux line (Curve D of Fig. 15) indicates the amount of the heat that is retained in the plate at any time increment.

Over-All Solution

The over-all solution for each parameter is a three-dimensional surface of the parameter versus time versus position along the plate channel element. Two parameters are of interest for the sample problem—surface heat flux and thermocouple temperature.

Surface Heat Flux

Surface heat flux is of interest because during a transient this parameter is not synonymous with heat generation. Figure 16 shows the code surface heat flux solution for the example problem. The region of forced convection is shown as the white-topped template portion of the solution nearest the zero time line. The local boiling region is shown with black-topped templates. Regions of heat transfer with surface temperatures in excess of T_{scrit} include the regions C, D, and E of Fig. 5. These regions are shown with the white-topped templates farthest from the zero time line. This figure shows, as a function of time, the propagation of the various regimes of heat transfer down the channel toward the inlet.

Thermocouple Temperature

The thermocouple temperature solution is of interest because this parameter will be checked with actual Bettis test measurements to determine the validity of the representation of surface flux (Fig. 5). Figure 17 shows the thermocouple temperature solution for the example problem. The designation of heat transfer regions is the same as for Fig. 16.

APPENDIX I: NOMENCLATURE

English Letter Symbols

A, C	constants in flux Eqs (38) and (39)	Btu/ft^2-hr
a	coolant heat pickup factor in Eq (17)	--
A_f	coolant cross-sectional flow area, UL	ft^2
A_p	plate area associated with node, $\Delta X\delta$	ft^2
a_1, a_4	constants in Eqs (46) and (47)	--
a_2, a_5	constants in Eqs (46) and (47)	lb/ft^2-hr
a_3	constant in Eqs (46) and (47)	lb^2/ft^4-hr^2
B, D	constants in flux Eqs (38) and (39)	Btu/ft^2-hr-°F
b	constant in flow Eq (24)	sec^{-1}
c	constant in enthalpy Eq (25)	Btu/lb-sec
C_p	specific heat at constant pressure	Btu/lb-°F
d	ordinary derivative	--
	constant in current Eq (26)	amp/sec

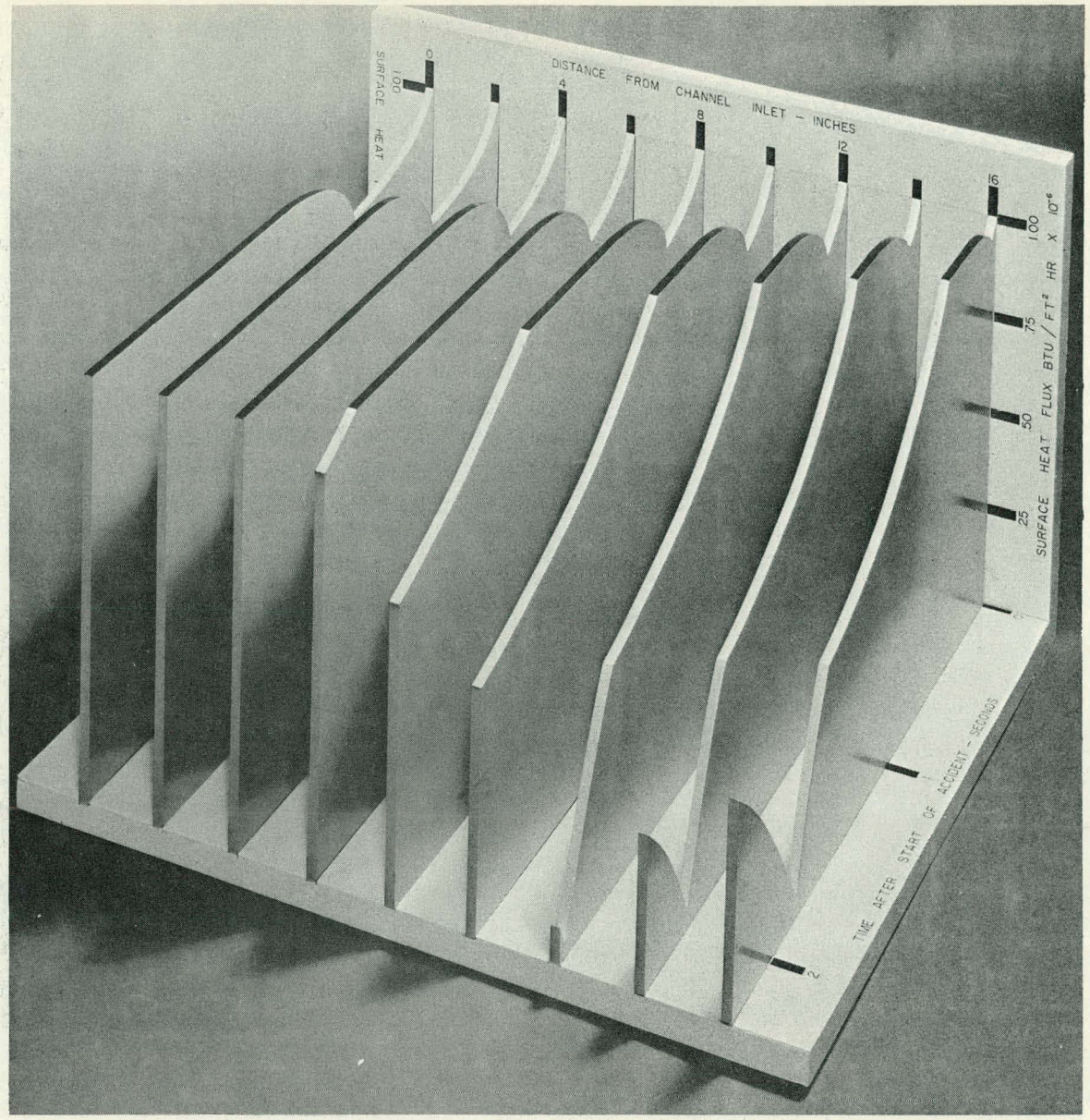

Fig. 16 Three-Dimensional Surface Flux Solution for Example Problem

D_H	hydraulic diameter, 4 A_f wetted paramcter	ft
e	constant in current Eq (26)	amp/sec
e_o	base of natural logarithms, 2.71828+	--
F	correlating function for H defined by Eq (32)	$Btu/(°F-[ft-hr]^{+0.2}-lb^{+0.8})$
f	friction factor	--
F_j	axial heat generation factor at node j	--
F_k	radial heat generation factor at node k	--
f_{iso}	isothermal friction factor	--
G	mass velocity	lb/ft^2-hr
g	gravitational acceleration constant	ft/hr^2
H	heat transfer coefficient	$Btu/ft^2-hr-°F$
h	coolant enthalpy	Btu/lb
$\bar{I}$	average specimen current	amp
K	thermal conductivity	$Btu-ft/ft^2-hr-°F$

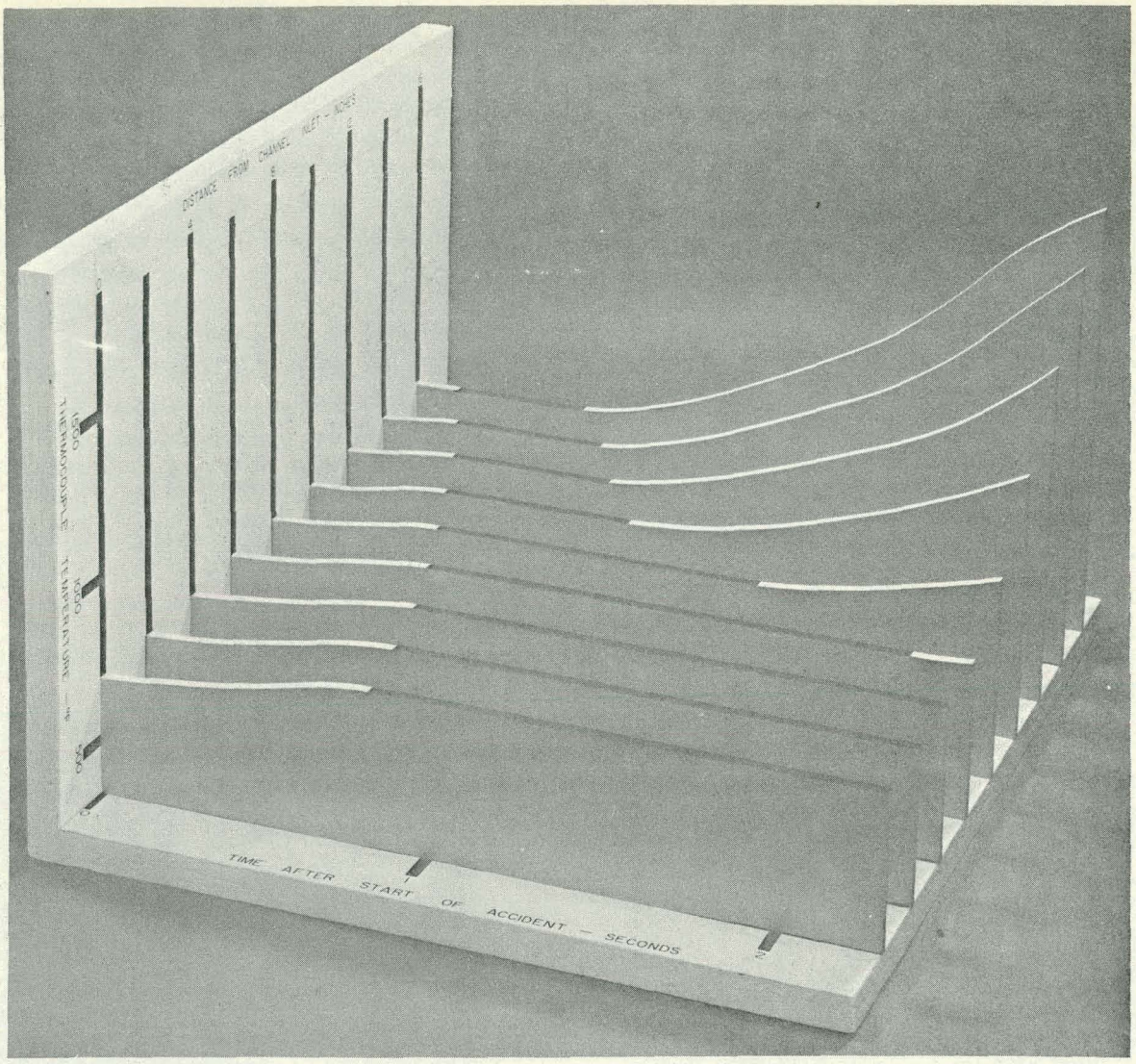

Fig. 17 Three-Dimensional Thermocouple Temperature Solution for Example Problem

L	channel thickness	ft
ℓ_a	distance from plate surface to farthest meat position	
ℓ_b	distance from plate surface to nearest meat position	
M	conversion factor for power	Btu/hr-watt
N'	next highest integer to $\Delta\tau_{plate}/\Delta\tau_{transport}$	--
N_F	number of radial generating nodes/plate side	-
P'	system pressure	psia
$\overline{P}$	average plate heat generation	Btu/hr
P_i	axial point to which region i extends	--
q'''	volumetric heat generation rate	Btu/ft^3-hr
R	electrical resistance of plate	ohm
T	temperature	°F
T'_{crit}	surface temperature at inception of film boiling	°F
T_{sat}	saturation coolant temperature	°F

T_{scrit}	surface temperature at inception of nucleate boiling	°F
U	channel width	ft
V	volume associated with node, $\Delta x \delta z$	ft^3
W	mass flow rate	lb/hr
X	coolant quality	--
x	number of nodes in x direction	--
	last node in x direction	--
	plate thickness direction	ft
Y	total plate thickness	ft
z	channel length direction	ft
	last node in z direction	--
z_j	length from inlet to node j	ft
$\Delta T_{J\&L}$	film drop required to cause local boiling	°F
ΔT_f	local film drop based on Dittus-Boelter coefficients of 0.030	°F
Δx	plate thickness represented by node	ft
Δz_i	mesh length in axial region i	ft
Δz_2	length from inlet to 1st downstream axial node	ft
$\Delta z'$	smallest axial length between successive nodes	ft
( )	denotes "function of"	--

Greek Letter Symbols

α	thermal diffusivity, $K_m/\rho_m C_{pm}$	ft^2/hr
δ	plate width	ft
Δ	finite difference form of derivative	--
ϵ	initialization convergence criterion	°F
η	summation index	--
μ	coolant viscosity	lb/ft-hr
ρ	density	lb/ft^3
ρ_E	electrical resistivity of plate	$ohm\text{-}ft^2/ft$
Σ	summation sign	--
τ	time	hr
τ'	time	sec
Φ^2_{Lo}	correlating factor for bulk boiling frictional pressure drop	--
ϕ	heat flux at plate surface	$Btu/ft^2\text{-}hr$
X_1, X_2	correlating factors for Φ^2_{Lo} defined by Eqs (45) and (46)	--

Dimensionless Groupings

N_{Nu}	Nusselt number, $(H D_H/K)$, heat transfer modulus
N_{Pr}	Prandtl number, $(C_p \mu/K)$, fluid property modulus
N_{Re}	Reynolds number, $(D_H G/\mu)$, flow modulus

Subscripts

Λ	spatial acceleration
DNB	departure from nucleate boiling flux as defined by Eqs (36) and (37)
E	elevation
f	frictional
fluid	fluid
i	time index

j	axial space index (z direction)
k	radial space index (x direction)
l	inlet position
m	metal
o	initial time
plate, P	plate
s	plate surface
sat	saturation
T	time acceleration
TC	thermocouple
Total	total
Transport	fluid transport
W	coolant

APPENDIX II: DERIVATION OF EQUATIONS

The development of the finite difference representation of the governing differential equations is given in this section.

Plate Equations

The governing plate conduction equation

$$\rho_m C_{pm} \frac{\partial T_m}{\partial \tau} = K_m \frac{\partial^2 T_m}{\partial x^2} + q''' (x, \tau) \tag{1}$$

is written as follows (refer to Fig. 2):

$$\frac{\Delta T_{ijk}}{\Delta \tau} = \frac{K}{\rho C_p} \frac{\Delta^2 T_{ijk}}{\Delta x^2} + \frac{q'''_{ijk}}{\rho C_p} , \tag{72}$$

where the metal, m, subscript has been dropped for simplicity. Examining a node, k, at time, i, the following approximations are made:

$$\Delta T_{ijk} \approx T_{ijk} - T_{i-1,jk} \tag{73}$$

$$\frac{\Delta^2 T_{ijk}}{\Delta x^2} \simeq \frac{1}{\Delta x} \left[\left. \frac{dT_{ijk}}{dx} \right| - \left. \frac{dT_{ijk}}{dx} \right| \right] \tag{74}$$

node interface nearest channel — node interface farthest from channel

The values of the temperature slopes at the two node interfaces are approximated as follows:

Internal Node, K

$$\frac{\Delta^2 T_{ijk}}{\Delta x^2} = \frac{1}{\Delta x} \left[\frac{T_{i-1,j,k-1} - T_{i-1,jk}}{\Delta x} - \frac{T_{i-1,jk} - T_{i-1,j,k+1}}{\Delta x} \right] \tag{75}$$

Last, x^{th}, Node

The slope representation is the same as for the internal node, K, above with the symmetry condition

$$T_{i-1,jx} \equiv T_{i-1,j,x+1} \tag{76}$$

With this condition, the equations becomes

$$\frac{\Delta^2 T_{ijx}}{\Delta x^2} = \frac{1}{\Delta x}\left[\frac{T_{i-1,j,x-1} - T_{i-1,jx}}{\Delta x}\right] . \tag{77}$$

Thermocouple, TC, Node

The node representation for the TC node is the same as (76) for the right side of the equation. With the approximation

$$\frac{\Delta^2 T_{ijTC}}{\Delta x^2} \approx \frac{\Delta^2 T_{ijx}}{\Delta x^2} , \tag{78}$$

the representation becomes

$$\frac{\Delta^2 T_{ijTC}}{\Delta x^2} = \frac{1}{\Delta x}\left[\frac{T_{i-1,j,x-1} - T_{i-1,jx}}{\Delta x}\right] . \tag{79}$$

First, 1st, Node

Forced Convection and Nucleate Boiling—For a known surface temperature, the expression for the first node becomes

$$\frac{\Delta^2 T_{ij1}}{\Delta x^2} = \frac{1}{\Delta x}\left[\frac{T_{i-1,js} - T_{i-1,j1}}{\Delta x/2} - \frac{T_{i-1,j1} - T_{i-1,j2}}{\Delta x}\right] . \tag{80}$$

DNB, Partial Film Boiling, and Film Boiling—The equation

$$T_{ij1} = X\,\overline{T}_{ij} - T_{ij2} - T_{ij3} \cdots T_{ijx} \tag{10}$$

expresses a heat balance in the plate where $\overline{T}_{ij}$ is determined from known surface heat flux and generation conditions by Eq (15).

Surface, S, Node

Forced Convection—By a heat balance on the 1st node, the surface conditions, with respect to the node, can be expressed as

$$\left.\frac{dT}{dx}\right|_{i-1,js} = -\frac{H_{ij}}{K}(T_{i-1,js} - T_{ijw}) . \tag{81}$$

With the approximation

$$\frac{\Delta^2 T_{ijs}}{\Delta x^2} \approx \frac{\Delta^2 T_{ij1}}{\Delta x^2} , \tag{82}$$

$$\frac{\Delta^2 T_{ijs}}{\Delta x^2} = \frac{1}{\Delta x}\left[-\frac{H_{ij}(T_{i-1,js} - T_{ijw})}{K} - \frac{T_{i-1,j1} - T_{i-1,j2}}{\Delta x}\right] . \tag{83}$$

Nucleate Boiling—The statement

$$T_{ijs} \equiv T_{scrit} \tag{12}$$

expresses the empirical relationship that the wall temperature remains essentially constant, regardless of h_z, for a local boiling surface condition.

DNB, Partial Film Boiling, and Film Boiling—The equation

$$T_{ijs} = T_{i-1,js} + T_{ij1} - T_{i-1,j1} \tag{13}$$

is derived directly from the approximation

$$\frac{\Delta T_{ijs}}{\Delta \tau} \approx \frac{\Delta T_{ijl}}{\Delta \tau} \tag{84}$$

The use of the above representations with the Fourier modulus equation,

$$\frac{(\Delta x)^2}{\alpha \Delta \tau} \equiv 3 \tag{16}$$

(selected to insure plate stability), yields the plate Eqs (6)-(13).

Average Plate Temperature

Forced Convection and Nucleate Boiling—The rigorous equation

$$\overline{T}_{ij} = \frac{1}{Y} \int_o^Y T(x,\tau)dx \tag{85}$$

is approximated by the average node temperature as given by Eq (14).

DNB, Partial Film Boiling, and Film Boiling—Equation (15) expresses the local change in average temperature resulting from the instantaneous difference between the local heat production,

$$\sum_{k=1}^{x} (q'''_{ijk} \Delta x)$$

and the local surface heat flux, ϕ_{ij}.

Fluid Equations

The fluid equations, as represented by Eqs (17)-(23) are obtained by direct replacement of derivatives by finite differences.

Input Forcing Functions

The functional form of the input, Eqs (24)-(26), was determined from consideration of the data to be obtained from the Bettis electrically-heated test specimens (Fig. 4a).

The derivation of Eq (27), based on Fig. 4b, is as follows. If the total test section current, $\overline{I}_i$, is known, the total power production in the generation region of the assembly is

$$\overline{P}_{i\ total} = M \overline{I}_i^2 R \ , \tag{86}$$

and the power production per generating region is

$$\overline{P}_{i\ region} = M \left[\frac{\overline{I}_i}{2N_F} \right]^2 R \tag{87}$$

since the total current is carried by plate regions on each side of the channel.

The resistance of an individual node is

$$R = \frac{\rho_E z}{\Delta x \delta} = \frac{\rho_E z}{A_p} \ , \tag{88}$$

and the volume of a node is

$$V = \Delta x \delta z = A_p z \ . \tag{89}$$

Thus, the volumetric generation per generating node is

$$\frac{\overline{P}_{i\ region}}{V} = \frac{M \rho_E}{4 A_p^2} \left[\frac{\overline{I}_i}{N_F} \right]^2 \equiv \overline{q}'''_i \ . \tag{27}$$

For non-electrical tests, an equivalent $\bar{q}_i'''$ must be known for the generating region and converted to $\bar{I}_i$ input through Eq (27).

ACKNOWLEDGMENTS

The formulation of the thermal transient analysis problem, as now stated in the Fortran F0020 code, has evolved over a period of several years. The principal contributions to this effort are acknowledged below.

Dr. J. A. Clark, of the University of Michigan, derived the basic differential equations used in the code.

Dr. N. R. Amundson, of the University of Minnesota, performed the original reduction of the differential equations to a numerical form suitable for problem solution and assisted in the formulation of the solution sequence philosophy.

The preliminary method feasibility and solution sequence studies were performed on THETA, a Wolontis 650 version of F0020. This work, including the coding, was performed by E. Quandt and J. S. Williams, Jr. of the Thermal and Hydraulics Section of Bettis Advanced Development and Planning Activities.

The Fortran 704 coding was performed by J. B. Callaghan, S. H. Meanor, and A. V. Pace of the Bettis Central Physics and Mathematics Department.

REFERENCES

1. S. O. Johnson, N. J. Curlee, and J. V. Reihing, "Simulation of Hot Channel Boiling in Water-Cooled Reactors," IRE Trans. on Nuclear Sci., Vol NS-5, No. 1 (1958), pp 1-9.
2. B. L. Anderson, T. J. Lawton, J. M. Weaver, and E. V. Somers, "ATBAC—An IBM-704 Code for Reactor Thermal Transients," WAPD-TM-20 (May 1957).
3. S. J. Green and J. S. Williams, Jr., "Fuel Element Temperature Response in the 'Beyond Burnout' Heat Transfer Region," WAPD-TH-414 (April 1958).
4. W. H. Jens and P. A. Lottes, "Analysis of Heat Transfer, Burnout, Pressure Drop, and Density Data for High Pressure Water," ANL-4627 (May 1951).
5. W. H. McAdams, Heat Transmission (New York: McGraw-Hill, 3rd ed., 1954).
6. R. A. DeBortoli, S. J. Green, B. W. LeTourneau, M. Troy, and A. Weiss, "Forced-Convection Heat Transfer Burnout Studies for Water in Rectangular Channels and Round Tubes at Pressure above 500 Psia," WAPD-188 (October 1958), Chap VI.
7. W. Milich and J. B. McDonough, "Progress Report 45 for February and March 1958," Section 1.2, "Film Boiling with Water Inside Tube," MSA Research Corporation (April 1958).
8. V. Paschkis, et al., "Quenching Program Technical Report 2, Summary of Experimental Results through July 1955," (Columbia University, Department of Mechanical Engineering Research Laboratories, August 1955).
9. B. W. LeTourneau and N. C. Sher, "Revised Pressure Drop Recommendations for Pressurized Water Reactor Design," WAPD-TH-326 (May 1957).
10. J. H. Keenan and F. K. Keyes, Thermodynamic Properties of Steam (New York: J Wiley & Sons, Inc., 1955).
11. E. J. Wellman, "A Survey of the Thermodynamic and Physical Properties of Water," Master's Thesis, Purdue University (January 1950).
12. T. C. Tsu and D. T. Beecher, Thermodynamic Properties of Compressed Water (New York: A. S. M. E., 1957).